

Artificial Intelligence-Enabled Multi-Scale Simulations for COVID-19 Drug Discovery

Arvind Ramanathan

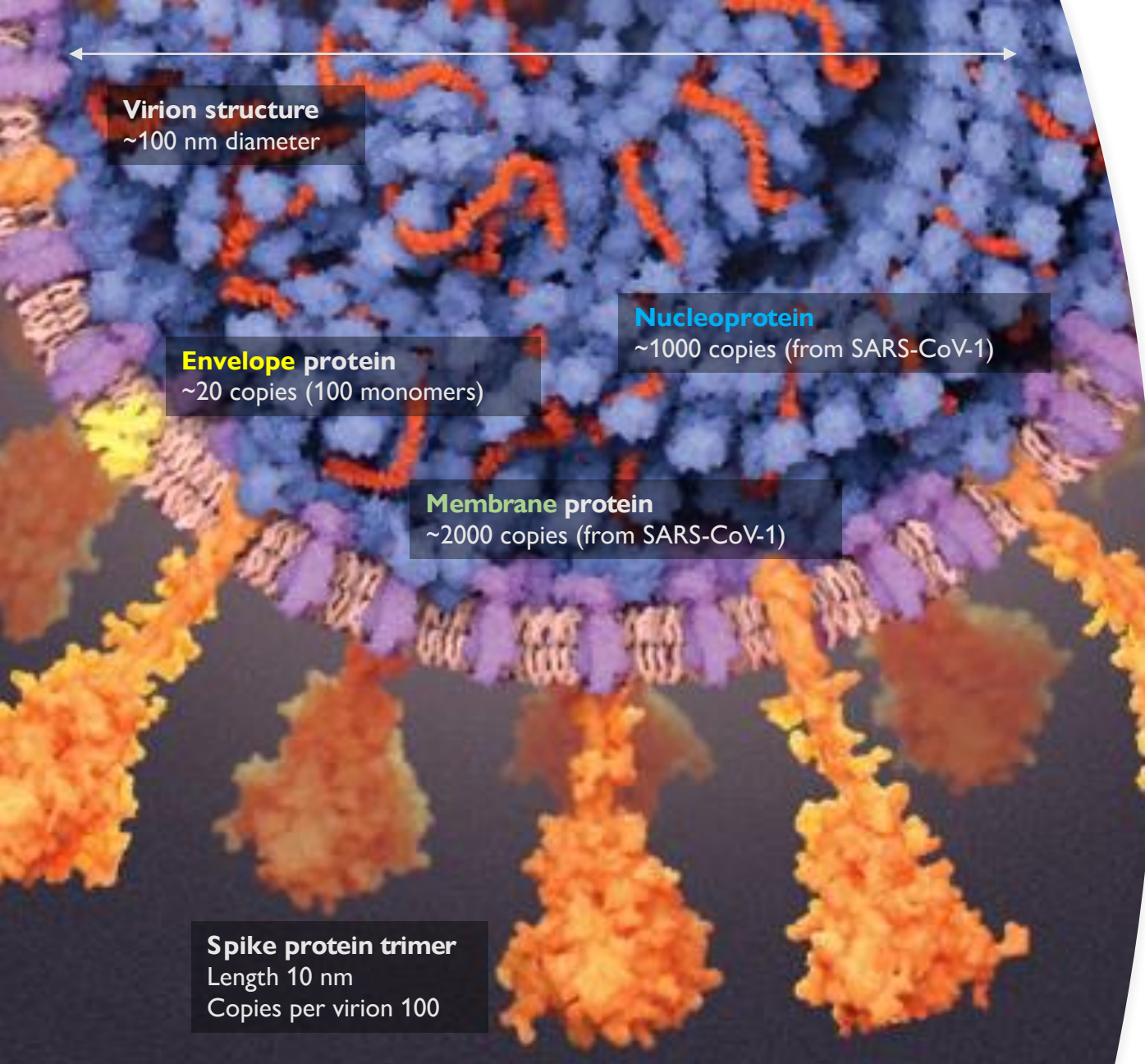
¹Data Science and Learning Division, Argonne National Laboratory

⁴University of Chicago

ramanathana@anl.gov | <https://ramanathanlab.org>

Some take home messages...

- AI/ML approaches can interface with rigorous physics-based methods to address drug discovery challenges
- Emerging AI/ML approaches impose interesting “co-design” requirements for HPC
 - on existing supercomputing platforms
 - on emerging heterogeneous platforms
- Discovery of novel biological aspects related to SARS-CoV-2
 - small molecules that can bind to and inhibit SARS-CoV-2
 - insights into how SARS-CoV-2 binds to the ACE2 receptor



Introduction to Covid-19 and SARS-COV-2

- Observed first in Wuhan (Dec 2019)
 - Quickly spread to the province of Hubei and then onto the world
- Spreads via close contact or through respiratory particles
- Virus is larger and far more stable than its counterparts (SARS and MERS)
 - can live on surfaces for a while
- Need a comprehensive strategy to identify small molecules (or other therapeutic strategies) to treat infection

Veronica Falconieri Hays; Source: Lorenzo Casalino, Zied Gaieb and Rommie Amaro, U.C. San Diego (*spike model with glycosylations*)

<https://www.scientificamerican.com/article/a-visual-guide-to-the-sars-cov-2-coronavirus/>

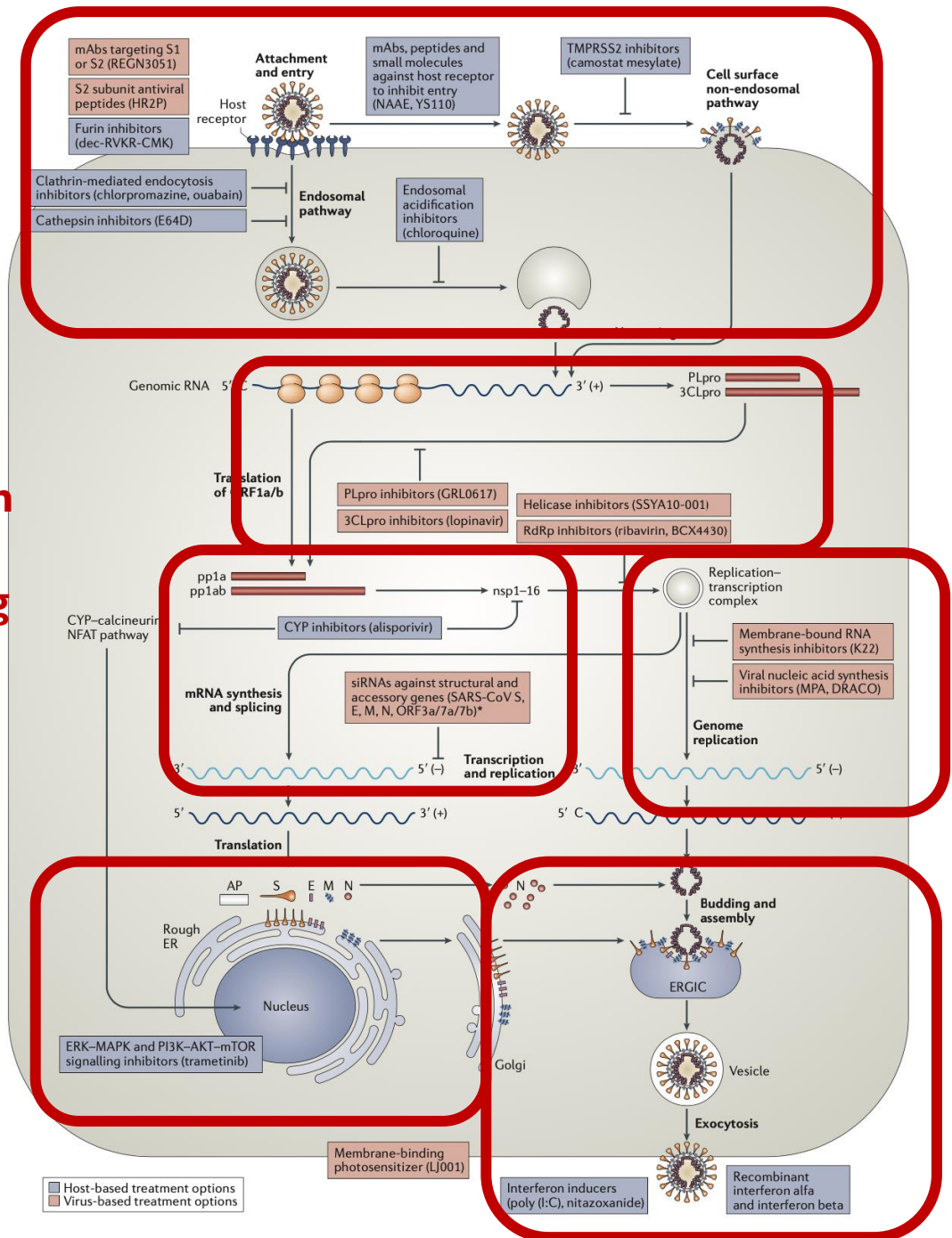
★ Structures solved at APS
 ★ Plausible Drug Targets
 ★ Priority Drug Targets

| Protein | Mol. weight (kDa) | Seq. similarity with SARS-CoV | Description |
|---------|-------------------|-------------------------------|--|
| Nsp1 | 19.8 | 91.1% | Suppresses host antiviral response |
| Nsp2 | 70.5 | 82.9% | |
| Nsp3 | 217.3 | 86.5% | Nsp3-Nsp4-Nsp6 complex involved in viral replication |
| Nsp4 | 56.2 | 90.8% | Nsp3-Nsp4-Nsp6 complex involved in viral replication |
| Nsp5 | 33.8 | 98.7% | Main protease (3C-like) |
| Nsp6 | 33.0 | 94.8% | Nsp3-Nsp4-Nsp6 complex involved in viral replication |
| Nsp7 | 9.2 | 100.0% | Nsp7-Nsp8 complex is part of RNA polymerase |
| Nsp8 | 21.9 | 99.0% | Nsp7-Nsp8 complex is part of RNA polymerase |
| Nsp9 | 12.4 | 98.2% | ssRNA binding |
| Nsp10 | 14.8 | 99.3% | Essential for Nsp16 methyltransferase activity |
| Nsp11 | 1.3 | 92.3% | Short peptide |
| Nsp12 | 106.7 | 98.3% | RNA polymerase |
| Nsp13 | 66.9 | 100.0% | Helicase/triphosphatase |
| Nsp14 | 59.8 | 98.7% | 3'-5' exonuclease |
| Nsp15 | 38.8 | 95.7% | Uridine-specific endoribonuclease |
| Nsp16 | 33.3 | 98.0% | RNA-cap methyltransferase |
| S | 141.2 | 87.0% | Spike protein, mediates binding to ACE2 |
| Orf3a | 31.1 | 85.1% | Activates the NLRP3 inflammasome |
| Orf3b | 6.5 | 9.5% | |
| E | 8.4 | 96.1% | Envelope protein, involved in virus morphogenesis and assembly |
| M | 25.1 | 96.4% | Membrane glycoprotein, predominant component of the envelope |
| Orf6 | 7.3 | 85.7% | Type I IFN antagonist |
| Orf7a | 13.7 | 90.2% | Virus-induced apoptosis |
| Orf7b | 5.2 | 84.1% | |
| Orf8 | 13.8 | 45.3% | |
| N | 45.6 | 94.3% | Nucleocapsid phosphoprotein, binds to RNA genome |
| Orf9b | 10.8 | 84.7% | Type I IFN antagonist |
| Orf9c | 8.0 | 78.1% | |
| Orf10 | 4.4 | - | |

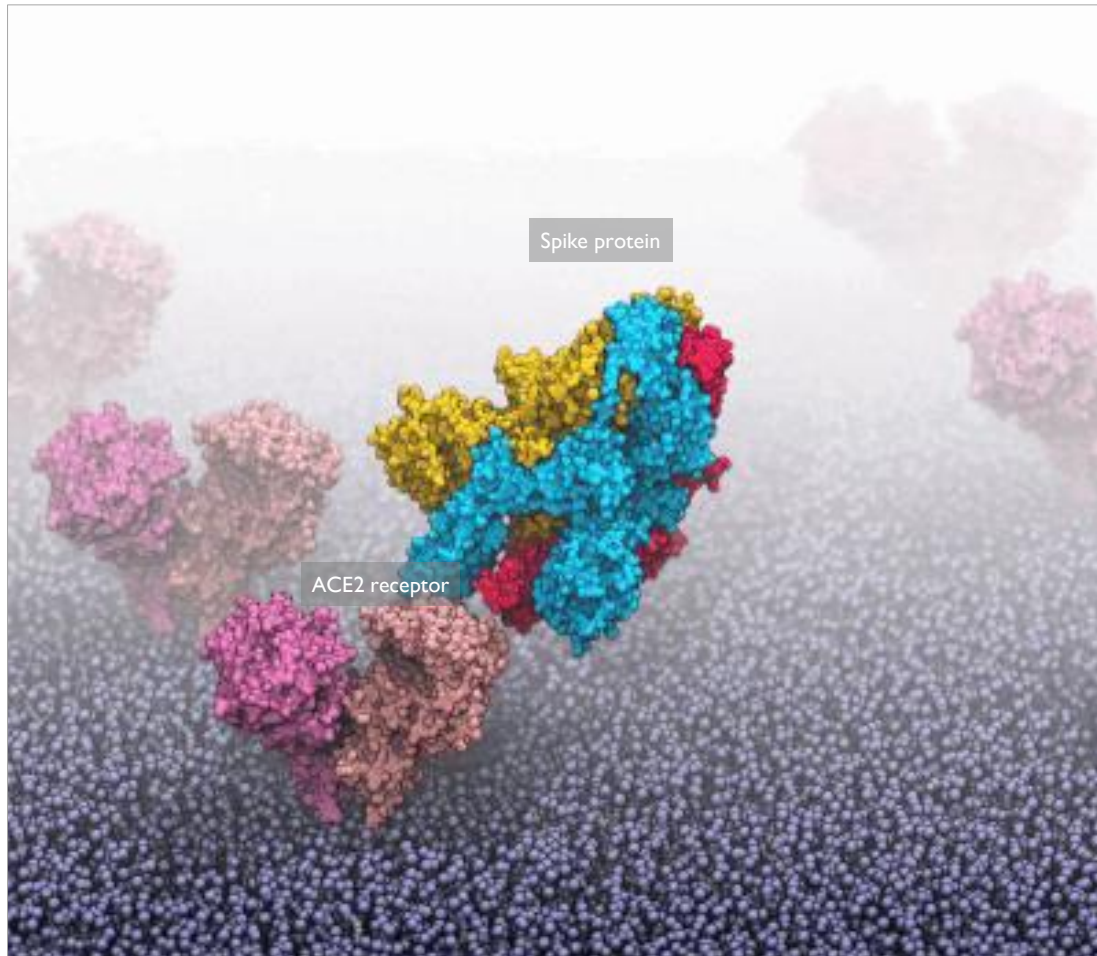
Viral Entry

Viral Replication and RNA Processing

Host Signaling Processes and Viral Exit



Outline (1)

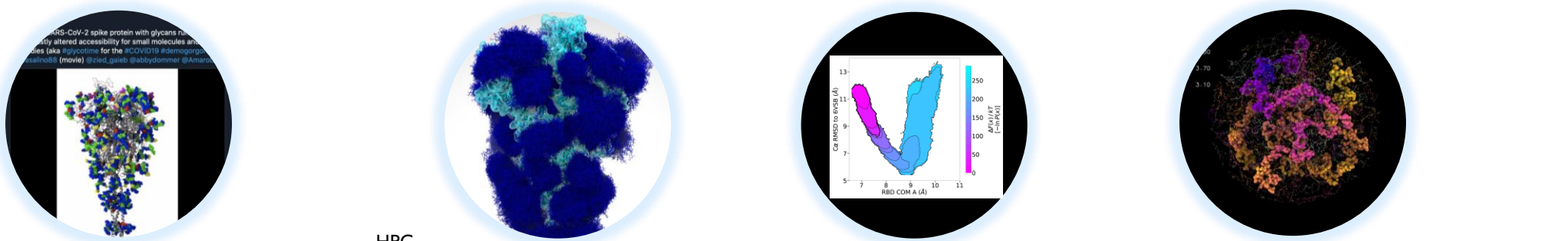


Simulations driven by AI depict how the CoV-2 spike protein attaches to the human ACE2 receptor protein
(Carlos Simmerling, Stony Brook)

How do we accelerate simulations of complex biological phenomena?

Collaboration between 10 institutions, 30 scientists across the globe!

Rommie Amaro
 Lillian Chong
 Shantenu Jha
 Tom Gibbs
 Syma Khalid
 Arvind Ramanathan



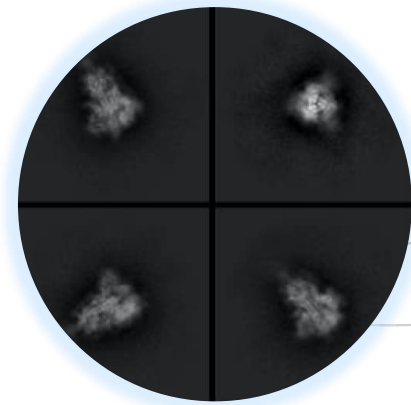
First Tweet

HPC Consortium Award

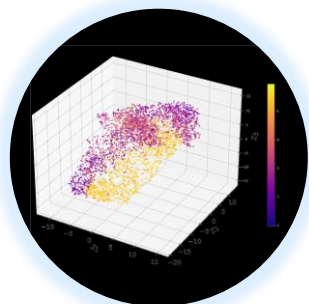
First Spike BioXriv

Large Ensemble Runs

CVAE Inference Finds Outliers and New States

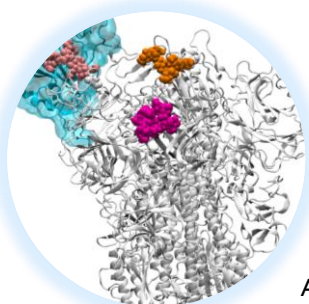


First CryoEM Images



First Test of CVAE Model

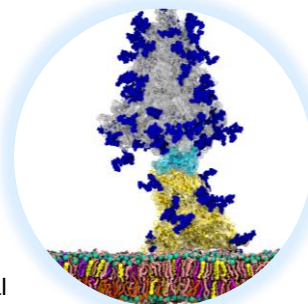
First Model Parallel CVAE Runs



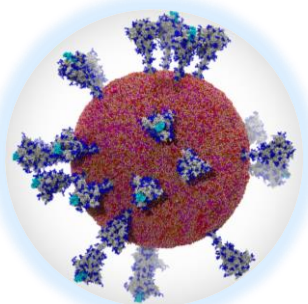
Early WE Runs

Adversarial CVAE Developed

Adversarial CVAE Trained w/ WE Data



8.5 Mn Atom Models



305 Mn Atom Model

February

April June

August

October

AI Enabled Key Feature Extraction



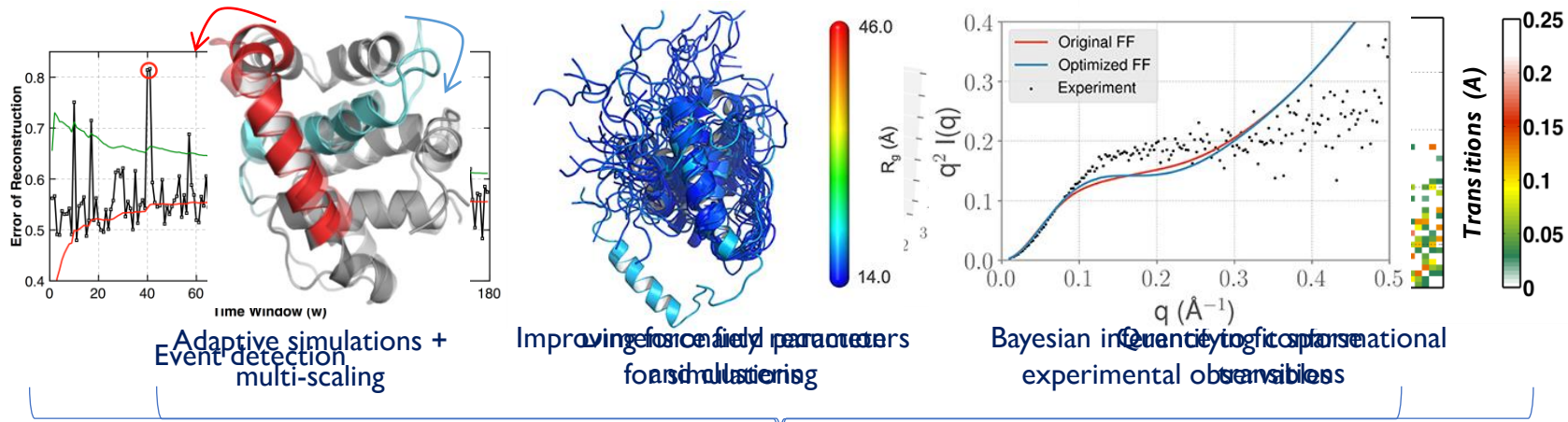
Large Model MD Simulation



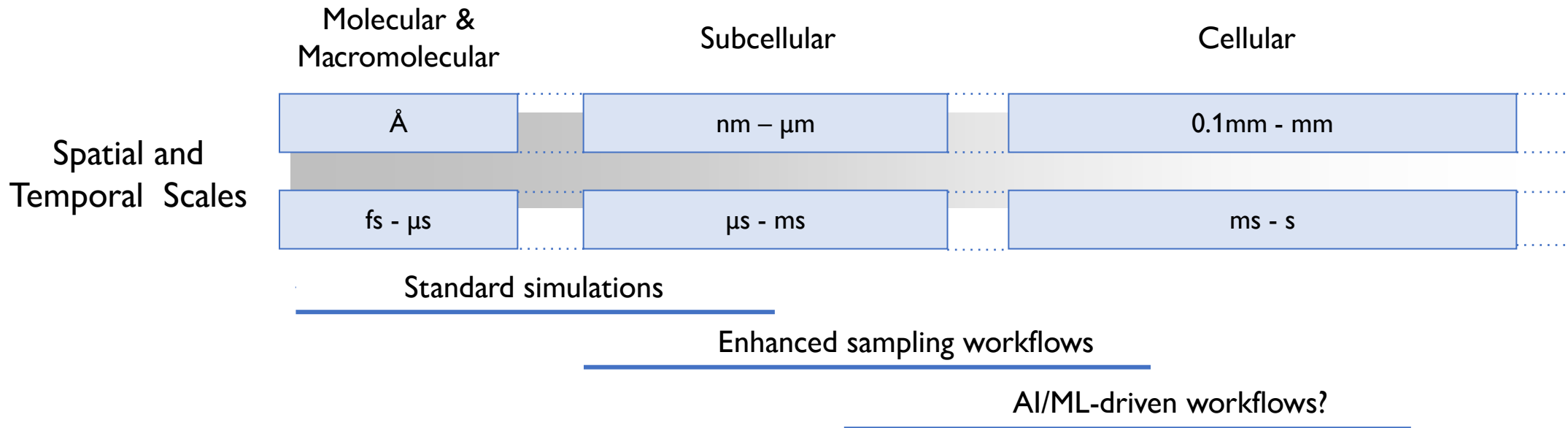
Weighted Ensemble Pathways



Statistical Inference: glue information across scales

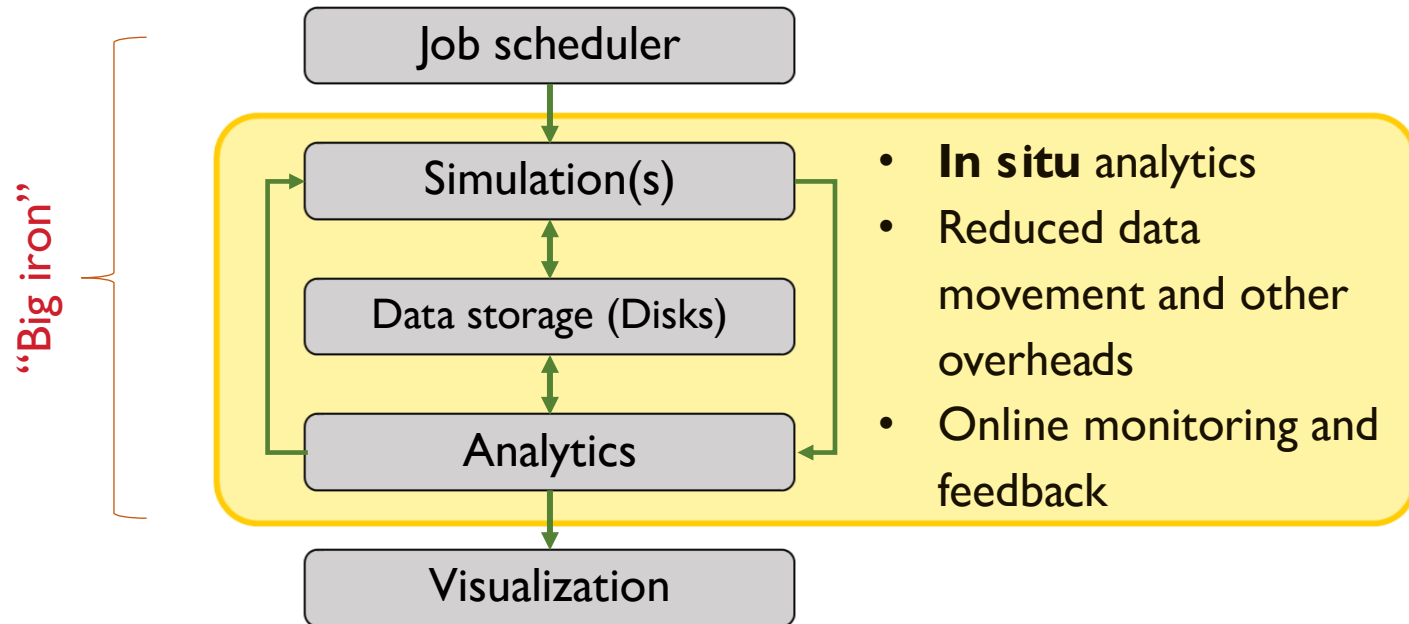


AI, probabilistic models, Bayesian inference



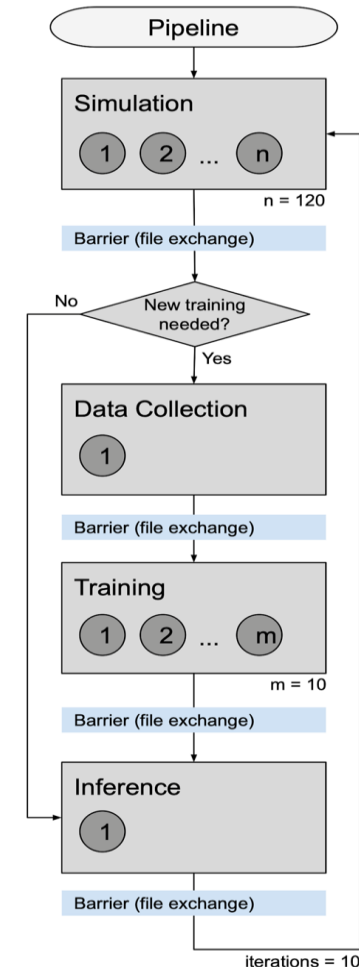
Standard simulation approaches face significant data movement and parallel analytics challenges

Need for interleaving analytics (AI/ML) + Simulations (HPC)



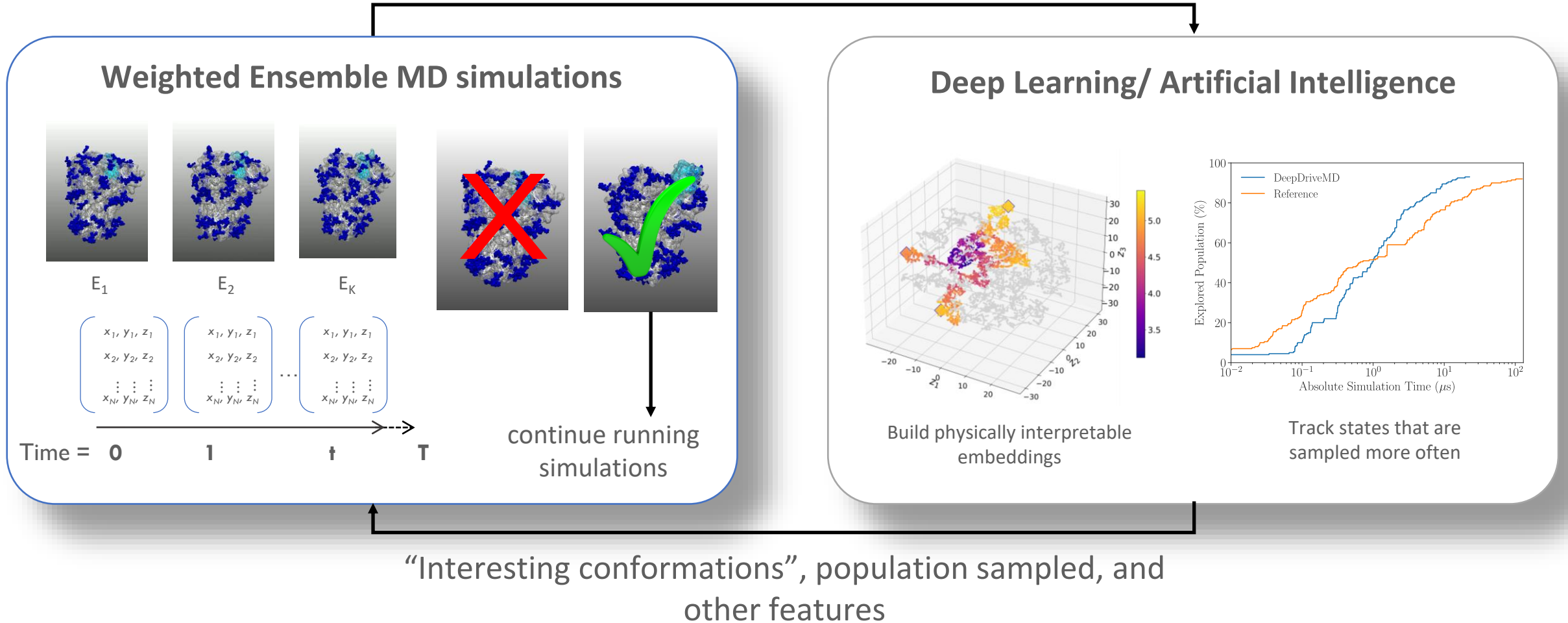
- Large simulations generate $> \mathbf{O(100\ TB)}$ of data
- Humanly impossible to peek into “biologically” interesting events!
- <http://deepdrivemd.github.io>
- Ma, Lee, et al. PARCO (2019)
- Lee, Ma, et al. Workshop on Deep Learning on Supercomputers, Supercomputing (2019)

Ensemble Toolkit Workflow



Combining AI with HPC: AI-driven MD simulations -- DeepDriveMD

Coordinates, contact maps, other features

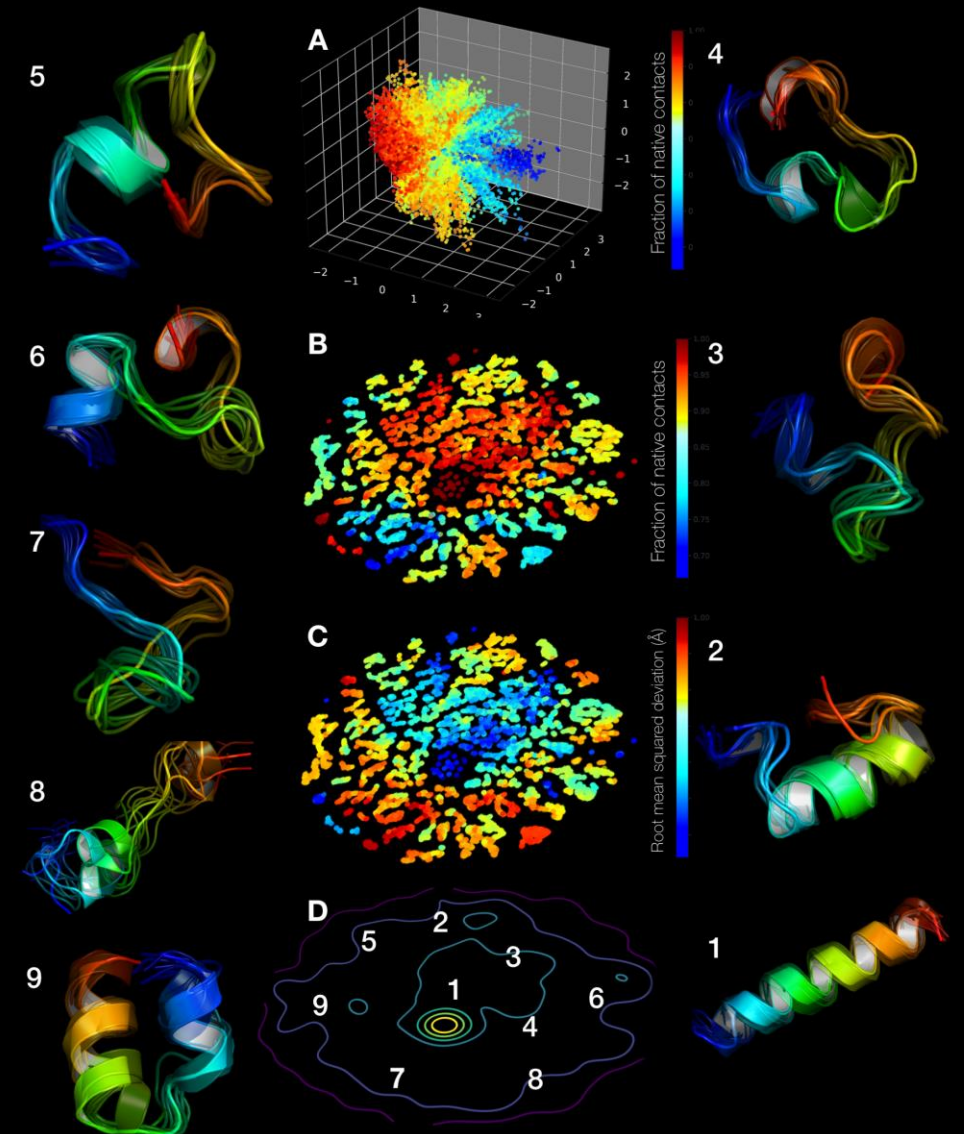


Learning Everywhere

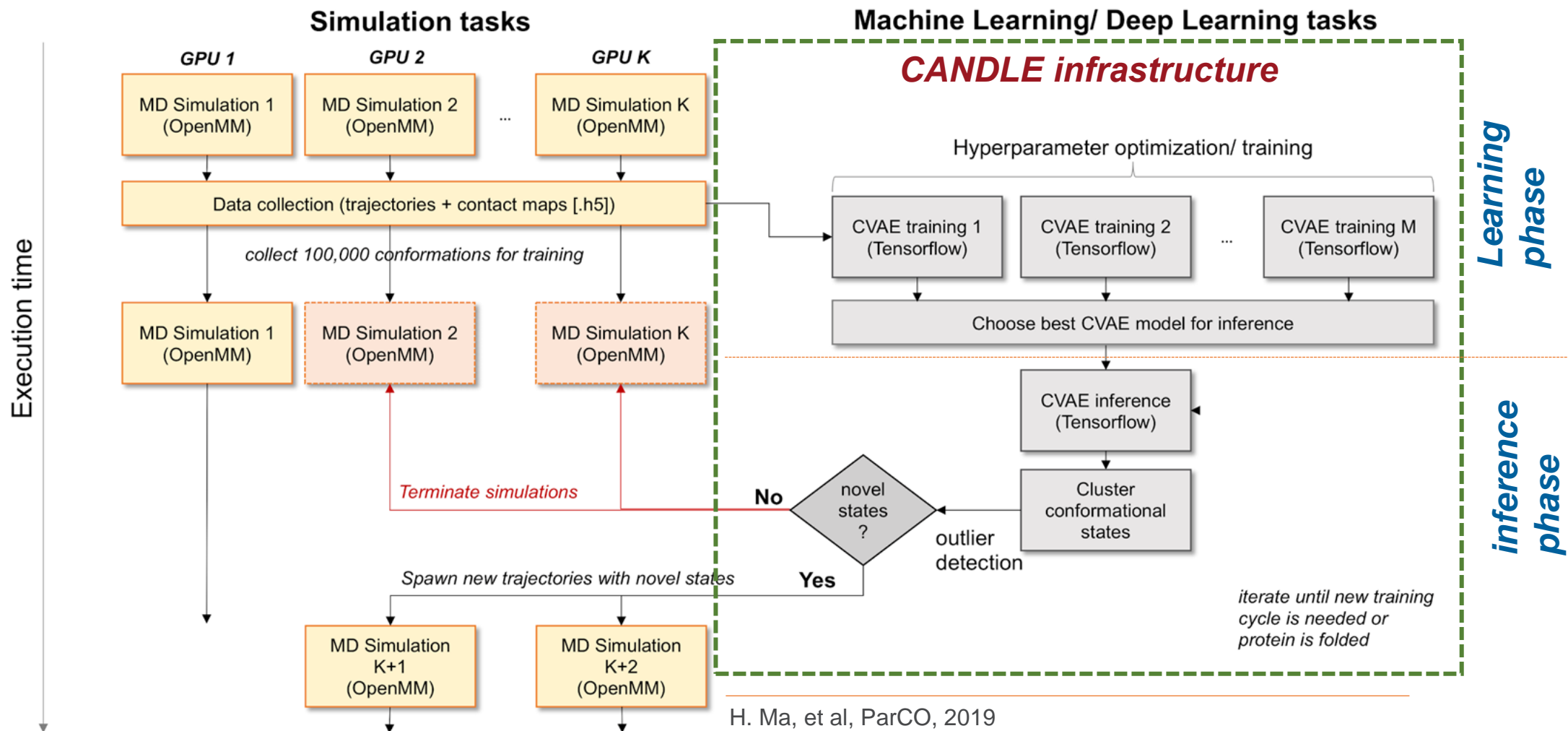
- Jha & Fox. In Visionary Track”, 15th International Conference eScience (2019), San Diego, California
- Jha & Fox. 15th International Conference eScience (2019), San Diego, California

Deep clustering of protein folding simulations

- ❑ Convolutional Variational Auto Encoders (CVAE)
 - ❑ Low dimensional representations of states from simulation trajectories.
 - ❑ CVAE can transfer learned features to reveal novel states across simulations
- ❑ On folding trajectories:
 - ❑ identify intermediate states in an unsupervised manner
- ❑ Applied across multiple protein systems can provide a general way to extract "reaction coordinates"



DeepDriveMD: DL driven Adaptive Ensembles MD



H. Ma, et al, ParCO, 2019

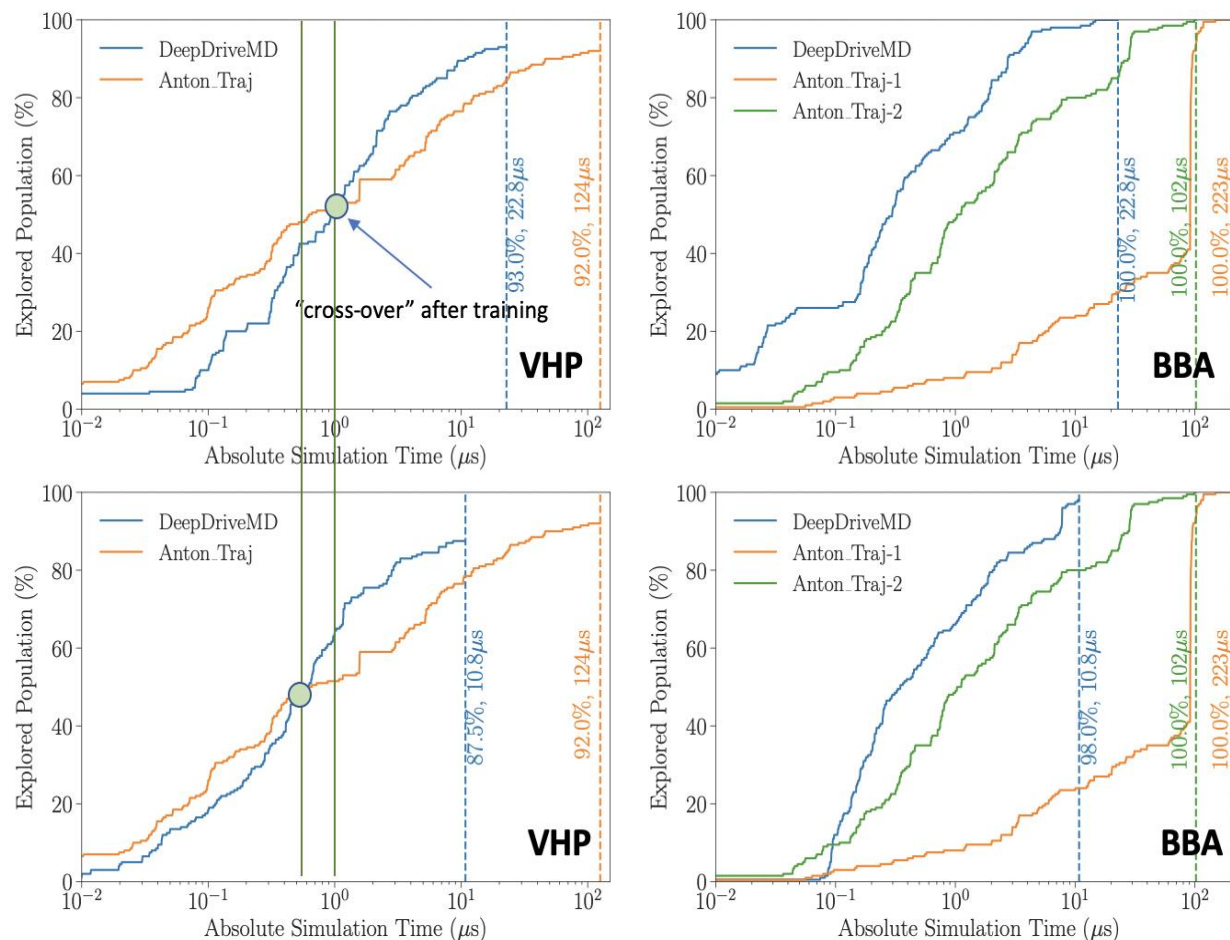
H. Ma, et al, Workshop on Deep Learning on Supercomputers, 2019

Collaboration with Shantenu Jha (Rutgers/ Brookhaven) and RADICAL team

DeepDriveMD is at least an order of magnitude better than traditional sampling

- Crossover point where DeepDriveMD based sampling is:
(i) accelerated (ii) improves over “classical” methods
- $O(100)$ greater sampling efficiency without considering time to train (for BBA protein)
 - If reference trajectories take $O(\text{microsecond})$ to sample a particular state, DeepDriveMD samples in $O(100 \text{ ns})$
 - For BBA, 98% sampled states are observed within 10 microseconds!
- Greater efficiency gains with larger proteins and complex dynamics
- Requires multiple and distinct levels of parallelism for “balanced” performance

DeepDriveMD: Deep-Learning Driven Adaptive Molecular Simulations for Protein Folding, Workshop on Deep Learning on Supercomputers, SC'19 <https://arxiv.org/abs/1909.07817>



SARS-CoV-2 Spike Protein

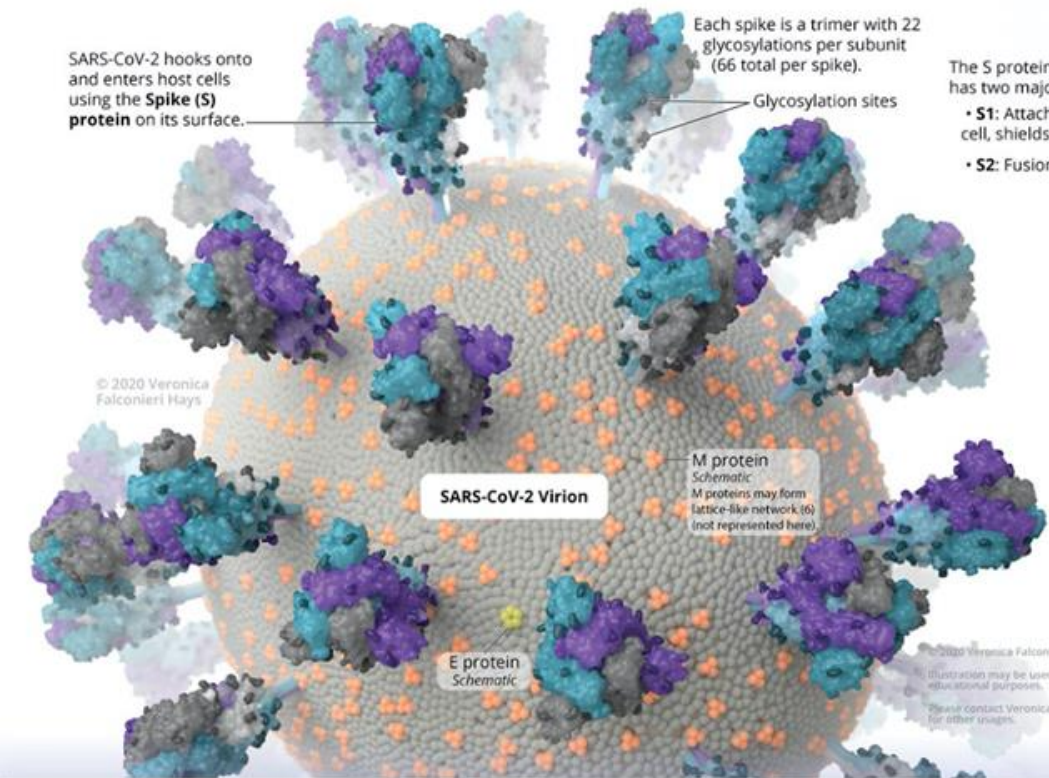
Structure and pre-fusion processing

Because of its location and function, the spike is the target of neutralizing antibodies, and the focus of vaccine design.

See something inaccurate? Please contact Veronica@FalconieriVisuals.com to let us know. Thank you!

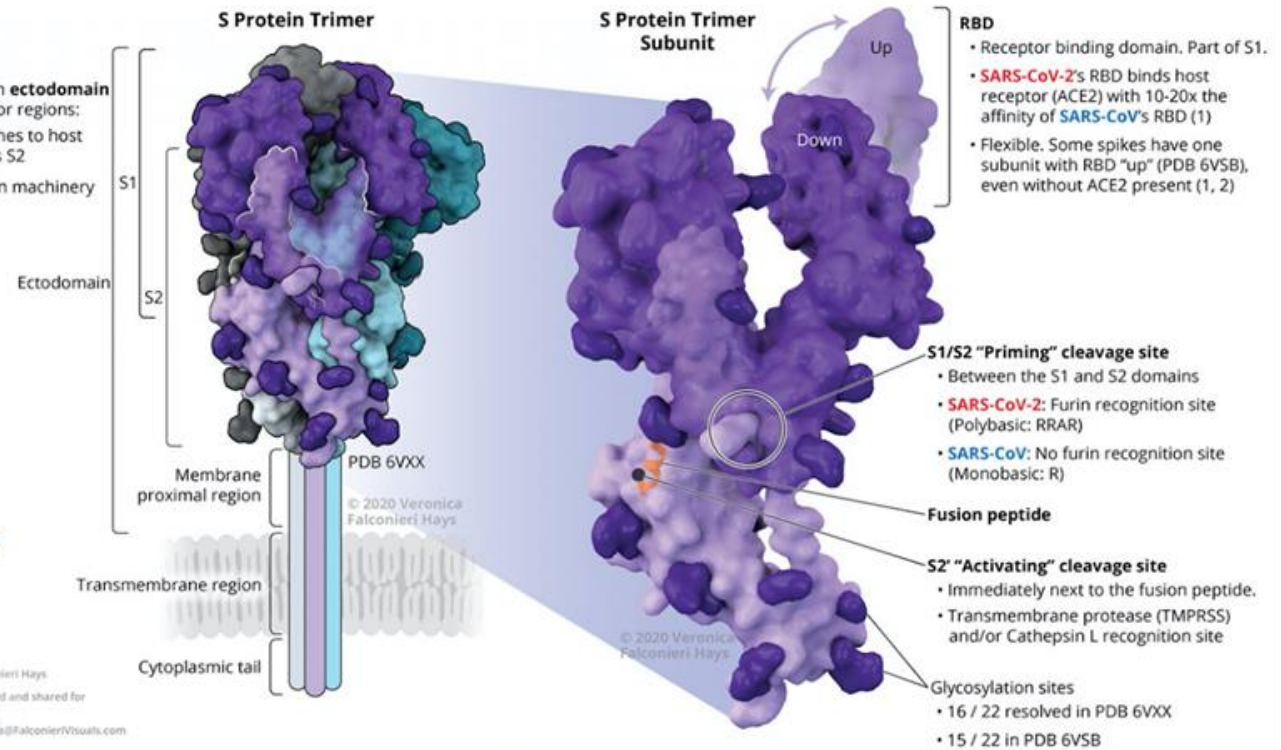
Last updated 4/2/2020

Abbreviations



The S protein **ectodomain** has two major regions:

- **S1:** Attaches to host cell, shields S2
- **S2:** Fusion machinery

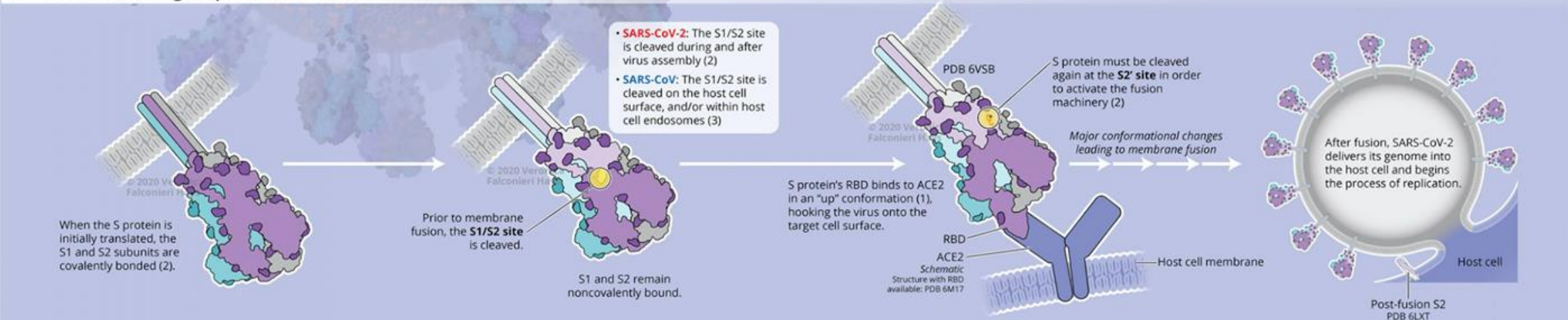


References

Spike Structure and Function

1. Wrapp D, Wang N, Corbett KS, Goldsmith JA, Hsieh C-L, Abiona O, et al. Cryo-EM structure of the 2019-nCoV spike in the prefusion conformation. *Science* (80-). 2020 Mar 13;367(6483):1260-3.
2. Walls AC, Park Y-J, Tortorici MA, Wall A, McGuire AT, Veesler D. Structure, Function, and Antigenicity of the SARS-CoV-2 Spike Glycoprotein. *Cell* [Internet]. 2020 Mar 6 [cited 2020 Mar 28]; Available from: <http://www.ncbi.nlm.nih.gov/pubmed/32155444>
3. Glowacka I, Bertram S, Muller MA, Allen P, Solleux E, Pfefferle S, et al. Evidence that TMPRSS2 Activates the Severe Acute Respiratory Syndrome Coronavirus Spike Protein for Membrane Fusion and Reduces Viral Control by the Humoral Immune Response. *J Virol*. 2011 May 1;85(9):4122-34. (SARS-CoV S1/S2 processing location)
4. Novel Coronavirus SARS-CoV-2: Transmission electron micrograph of SARS-CoV-2 virus particles, isolated from a patient. NIAID. Available from: <https://www.flickr.com/photos/niaid/49645120251/in/album-72157712914621487/>
5. Coronavirus illustration by David S. Goodsell, RCSB Protein Data Bank; doi: 10.2210/rcsb_pdb/goodsell-gallery-019. Available from: <http://pdb101.rcsb.org/sci-art/goodsell-gallery/coronavirus>
6. Neuman BW, Adair BD, Yoshioka C, Quispe JD, Circa G, Kuhn P, et al. Supramolecular Architecture of Severe Acute Respiratory Syndrome Coronavirus Revealed by Electron Cryomicroscopy. *J Virol*. 2006 Aug 15;80(16):7918-28. (SARS-CoV data: Size, S, M, and E protein stoichiometry)
7. Siu YL, Teoh KT, Lo J, Chan CM, Kien F, Escroun N, et al. The M, E, and N Structural Proteins of the Severe Acute Respiratory Syndrome Coronavirus Are Required for Efficient Assembly, Trafficking, and Release of Virus-Like Particles. *J Virol*. 2008 Nov 15;82(22):11318-30. (M protein SARS CoV)
8. Torres J, Parthasarathy K, Lin X, Saravanan R, Kukol A, Ding XL. Model of a putative pore: The pentameric α -helical bundle of SARS coronavirus E protein in lipid bilayers. *Biophys J*. 2006;91(3):938-47. (E protein SARS CoV)

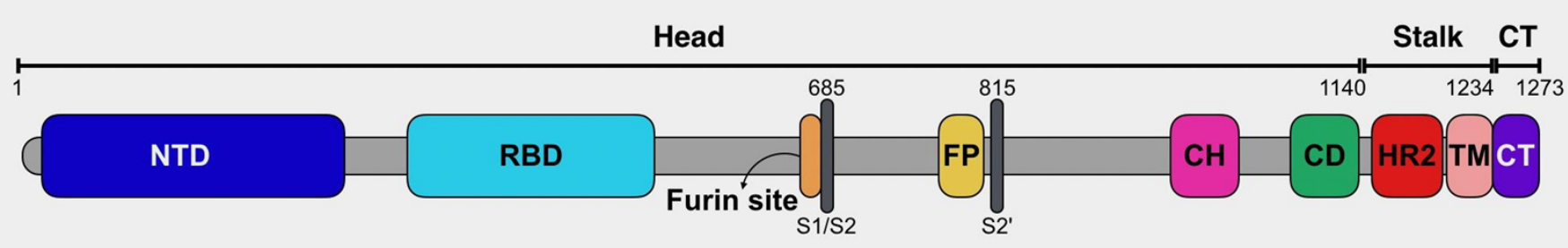
S Protein Processing Required for Fusion



Host cell membrane

Host cell

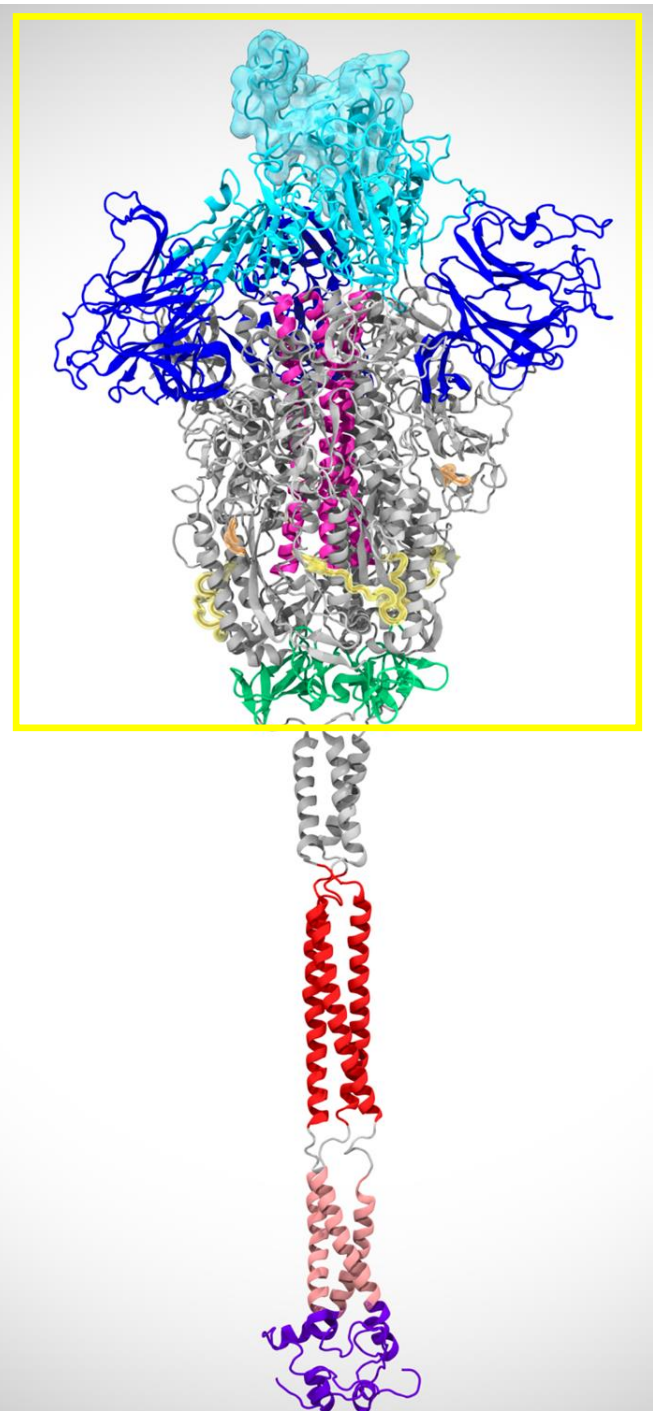
ACE2 Schematic Structure with RBD available: PDB 6M17



SARS-CoV-2 Spike sequence

Sequence of 6vsb (with gaps):

| | N-terminal | 10 | 15 | 20 | 30 | 40 | 50 | |
|----------------------------------|------------|-----------------------|----------------------|--------------------|---------------------------------------|-------------|-----------------|--------------------------------|
| SPIKE_COV2.BL0...principal chain | 1 | MFVFLVLLPLVSSQC | VNLT | TRTQLPPAYTNS | SFTRGVYYPDKVFRSSVLHS | | | S1 (14 to 685) |
| SPIKE_COV2.BL0...principal chain | 51 | TQDLFLPFFSNVTWFHAIHVS | GTNGTKRFDNPVLPFNDGVY | FASTEKSN I | | | | Signal peptide (1 to 13) |
| SPIKE_COV2.BL0...principal chain | 101 | IRGWI FGTTLD SKTQSL I | VN NATNVV I | KVCE FQFCNDPFLGVY | YHKNNK | | | |
| SPIKE_COV2.BL0...principal chain | 151 | SWMESEFRVYSSANNCTFEY | V SQPFLMDLE | GKQGNFKNLREFVKN | IDGY | | | |
| SPIKE_COV2.BL0...principal chain | 201 | FKIYSKHTP I | NLVRDL PQGFS | ALEPLVDLP I | GINITRFQTL LALHRSYLT | | | |
| SPIKE_COV2.BL0...principal chain | 251 | PGDSSSGWTA | GAAAYYVGYLQ | PRTFLLKYNENGTITDAV | CDALPLSETK | | | |
| SPIKE_COV2.BL0...principal chain | 301 | CTLKSFTVEK | G IYQTSNFRV | QPTES I | VRFPNITNLCPFGEVFNATRFASV | | | RBD |
| SPIKE_COV2.BL0...principal chain | 351 | YAWNRRKRI | SN CVADYSVL | YNSASFSTFKCY | GVSP TKLNDLCFTNVYADSF | | | |
| SPIKE_COV2.BL0...principal chain | 401 | VIRGDEV RQI | APGQTGKIAD | YNYKLPDDFT | GCVI AWNSNND SKVGGNYN | | | |
| SPIKE_COV2.BL0...principal chain | 451 | YLYRLFRKSN | LKP FERDI | STE IYQAGSTP | CNGVEGFNCYFPLQSYGFQPT | | | |
| SPIKE_COV2.BL0...principal chain | 501 | NGVGYQPYRV | VVLS FELLH | APATVCGPKKS | TNLVKNKCVNFNFGLTGTG | | | |
| SPIKE_COV2.BL0...principal chain | 551 | VLTESNKKFL | PFQFGRDIA | DTTDAVRDPQ | TLEILDITPCSF GGVSVITP | | | |
| SPIKE_COV2.BL0...principal chain | 601 | GTNTSNQVAV | LYQDVNCTE | VPVAIHADQLT | PTWRVYSTGNSVFQTRAGCL | | | |
| SPIKE_COV2.BL0...principal chain | 651 | IGAEHVNSY | ECDIPIGAGI | CASYQTQNTS | PRRAF ⁶⁸⁵ SVASQSI IAYTMSLG | | | Furin site S1/S2 cleavage site |
| SPIKE_COV2.BL0...principal chain | 701 | AENSVAYSNN | SIPTNFTIS | VTTEILPVS | MTKTSVDCTMYICGDS TECS | | | S2 (686 to 1273) |
| SPIKE_COV2.BL0...principal chain | 751 | NLLLQYGSF | CTQLNRALT | GIAVEQDKNT | QEVFAQVKQIYKTPPIKDFGGF | | | |
| SPIKE_COV2.BL0...principal chain | 801 | NFSQILPDP | SKPSKRSF | IEDLLFNKV | TADAGFIKQYGDCLGDI AARDLI | | | |
| SPIKE_COV2.BL0...principal chain | 851 | CAQKFNGL | TVLPPLLT | DEMIAQYTS | ALLAGTITSGWTFGAGAA LQIPFAM | | | |
| SPIKE_COV2.BL0...principal chain | 901 | QMAYRFNG | IGVTQNV | LYENQKLI | ANQFNSAIGKIQDSLSTASALGKLQD | | | |
| SPIKE_COV2.BL0...principal chain | 951 | VVNQNAQAL | NLTLVKQL | SSNFGA | ISSVLNDILSRLDKVEAEVQIDRLITGR | | | |
| SPIKE_COV2.BL0...principal chain | 1001 | LQSLQTYV | TQQLIRAAE | IRASANLAAT | KMSECVLGQSKRVDFCGKGYHLM | | | |
| SPIKE_COV2.BL0...principal chain | 1051 | SFPQSAPHG | VFLHVTV | YVPAQ | EKNFTTAPAI | CHDGHKAFP | REGVFVSNGT | |
| SPIKE_COV2.BL0...principal chain | 1101 | HWFVTQRNF | YEPQIIT | TDNTFVSGN | CDVVI | GIVNNTVYDP | LQPELDSFKE | |
| SPIKE_COV2.BL0...principal chain | 1151 | ELDKYFKN | H TSPDVL | LDGDIS | GINASVVNI | QKEIDRLNEVA | KNLNESLIDL | |
| SPIKE_COV2.BL0...principal chain | 1201 | QELGKYE | QYIKWP | WYIWLGF | IAGLIA | IVMVTIML | CCMTSCCSCLKGCSC | |
| SPIKE_COV2.BL0...principal chain | 1251 | GSCCKF | DEDDSE | PV | LKGVK | LHYT | | |



Weighted Ensemble (WE) method

- From Huber and Kim *Biophys. Journal* (1996)
- Instead of running one long simulation, runs many short simulations (“walkers”) with probabilities
- Samples the free energy landscape defined by chosen progress coordinates □ landscape is divided into “bins” and user chooses which trajectories to continue based on how they are progressing
- Trick is that you miss out on the ‘waiting times’ or the dwell times in energy wells for molecular events

- Why use the WE method?
 1. No statistical bias is added to the system
 2. Can sample **both** thermodynamic and kinetic properties
 3. Continuous, unbiased pathways can be obtained
 4. Monitoring evolution and convergence of properties is possible
 5. Adjusting bins and other parameters “on-the-fly” is possible

Weighted Ensemble Simulations

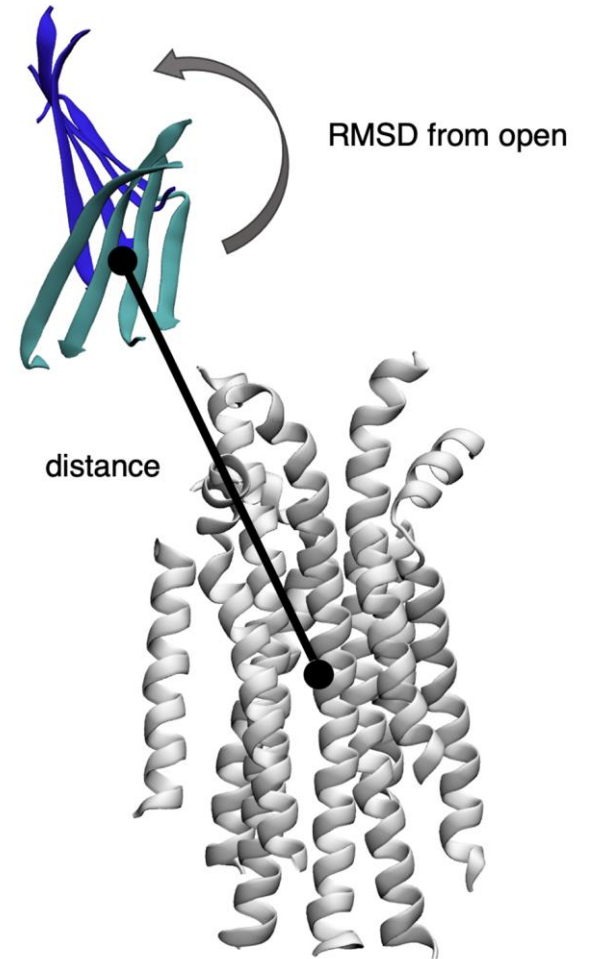
- ~ 600,000 atoms, the largest system **by an order of magnitude** that has been simulated using the WE method
- Initial state: 6VXX (closed)
- Weighted Ensemble Simulation Toolkit with Parallelization and Analysis (WESTPA)
- Initial runs on SDSC Comet, NVIDIA P100 GPUs
- Longhorn system at the Texas Advanced Computing Center (TACC)
- AMBER 18 MD engine, GPU optimized pmemd.cuda on 100 NVIDIA V100 GPUs

Aggregate sampling: ~200 microseconds actual simulation time

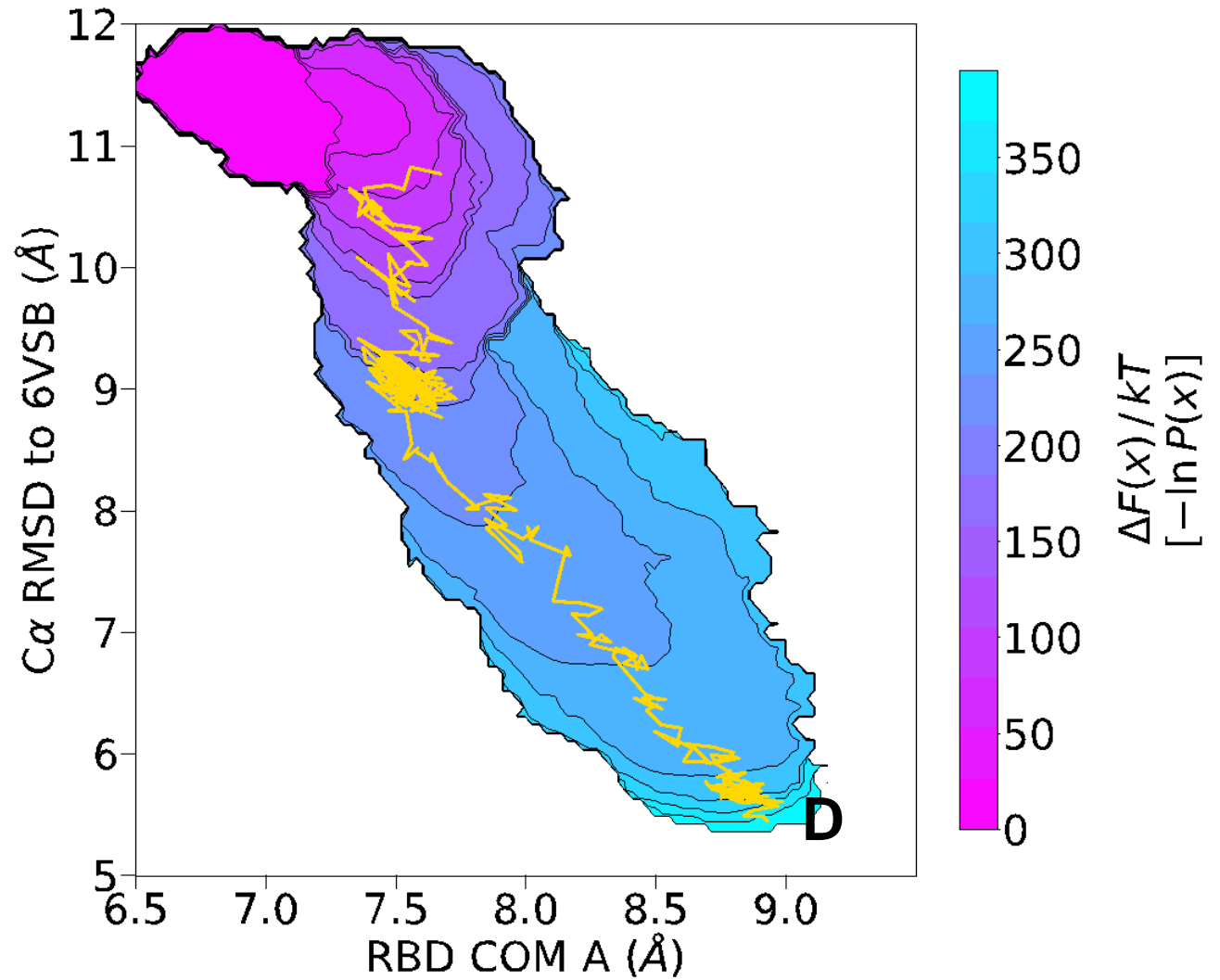
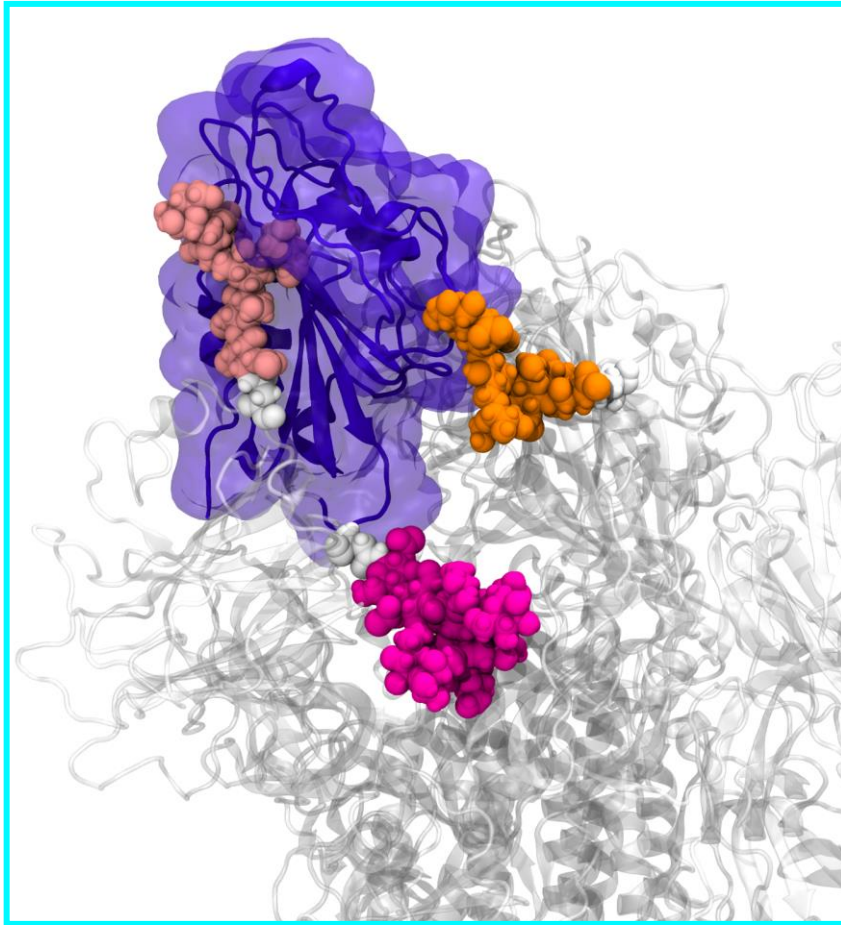
Equivalent of ~ 100s of milliseconds of timescale sampling with WE

~ 100TB of data with compression, w/o solvent (protein only)

Collaboration with Terra Stzain, Shirley Ahn, Antony Bogetti, Lillian Chong



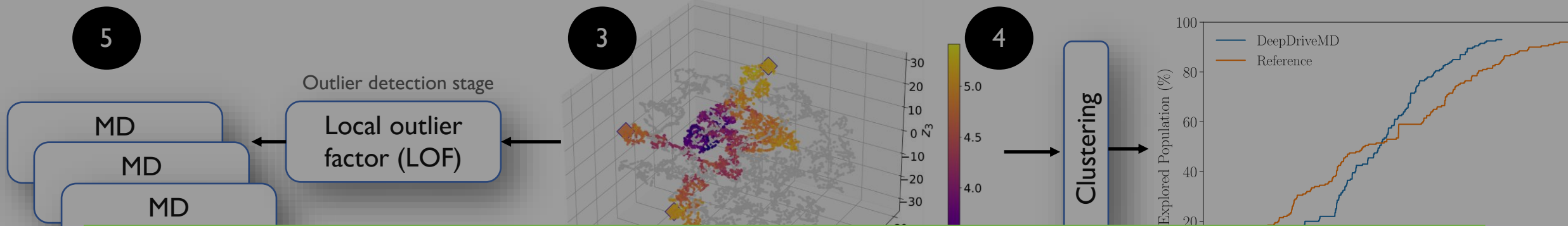
Continuous unbiased spike opening



Collaboration with Terra Stzain, Shirley Ahn, Antony Bogetti, Lillian Chong

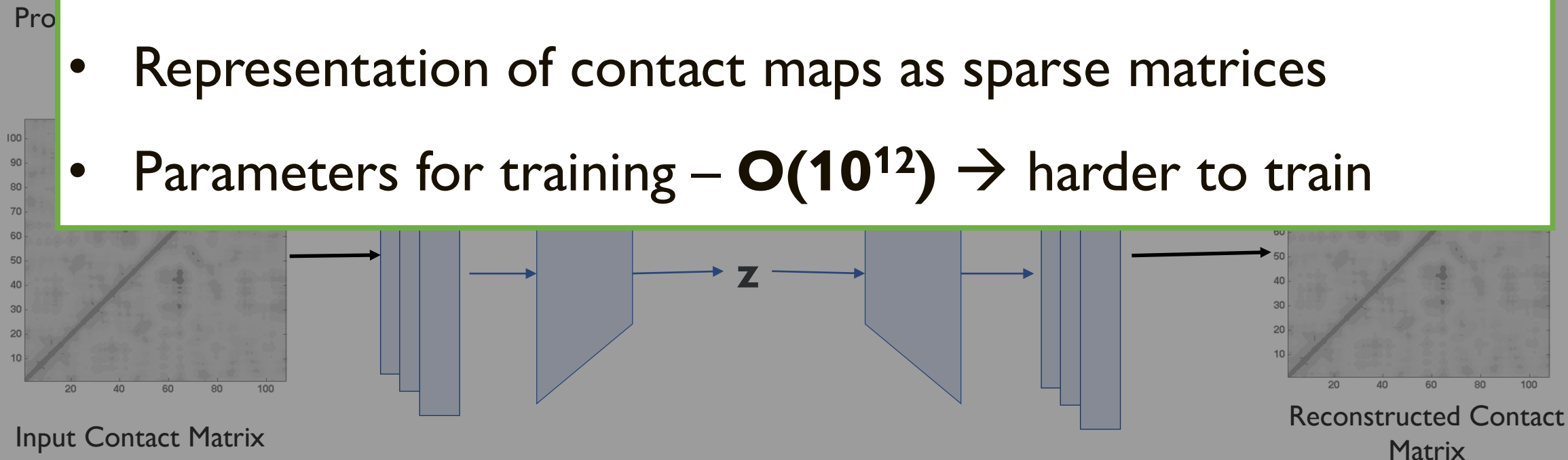
Interesting conformational states sampled

Tracking conformational states sampled



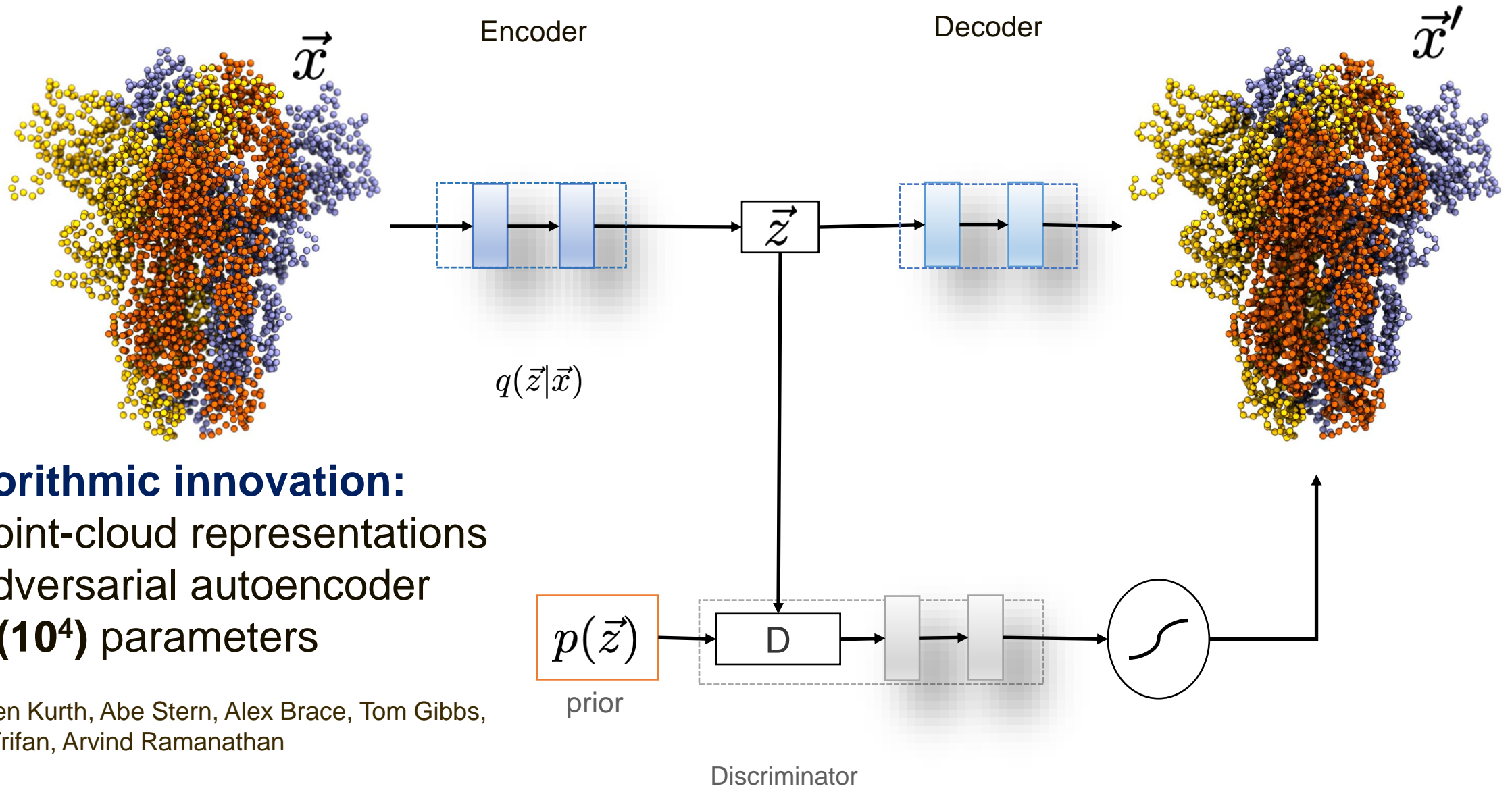
Computational challenges

- Representation of contact maps as sparse matrices
- Parameters for training – $\mathcal{O}(10^{12}) \rightarrow$ harder to train



- Bhowmik, Gao, et al. BMC Bioinformatics (2018)
- Romero, Ramanathan, et al. Proc. Natl. Acad. Sci. USA (2019)

Adversarial autoencoders for efficient analysis

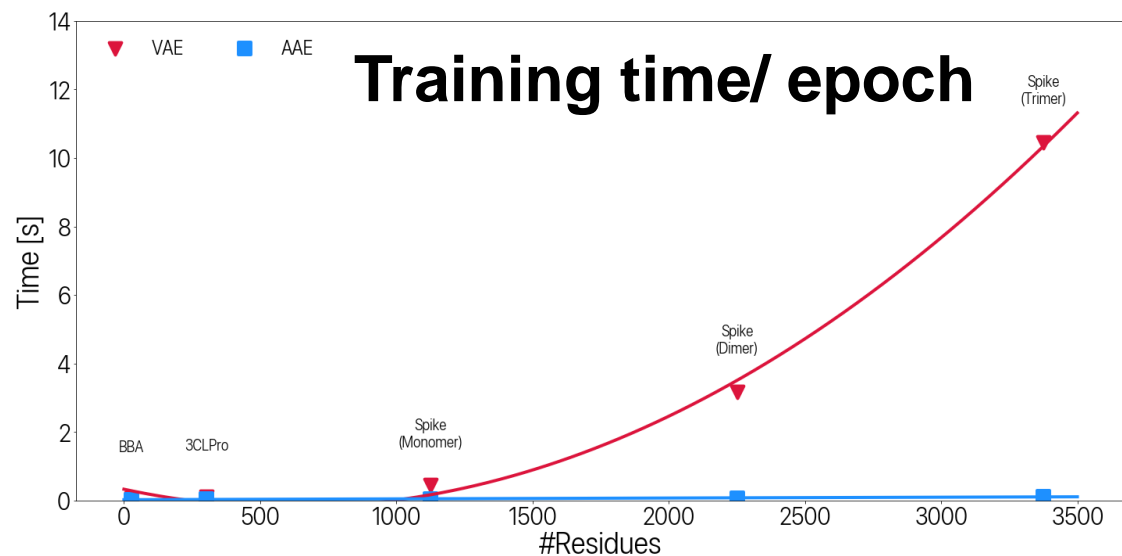
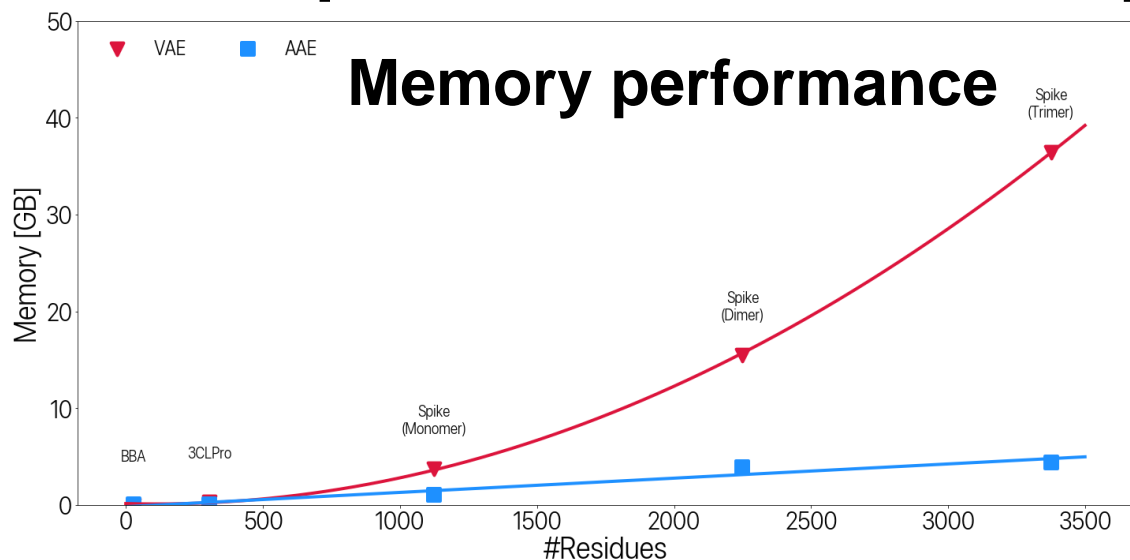


Algorithmic innovation:

- Point-cloud representations
- Adversarial autoencoder
- $\mathbf{O}(10^4)$ parameters

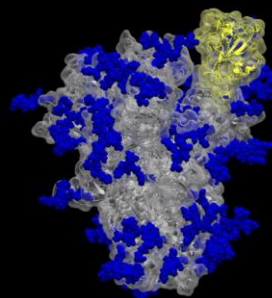
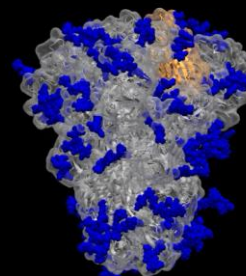
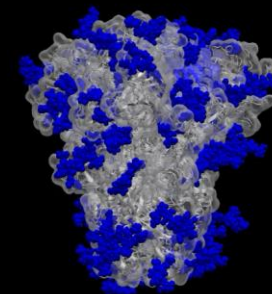
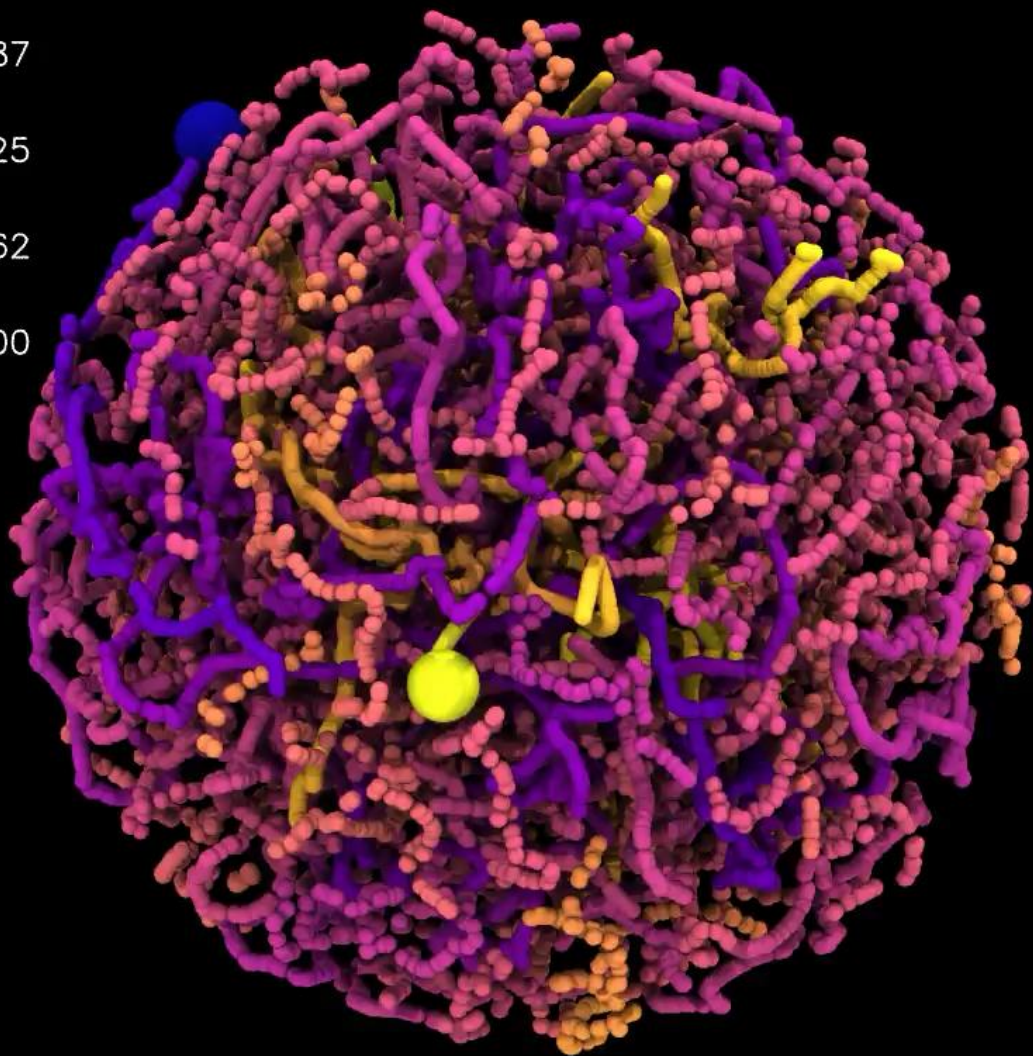
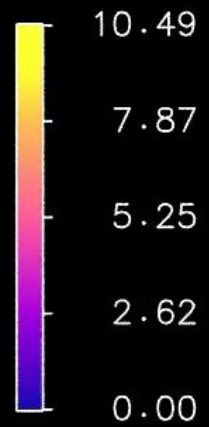
Thorsten Kurth, Abe Stern, Alex Brace, Tom Gibbs,
Anda Trifan, Arvind Ramanathan

DeepDriveMD: Computational Performance

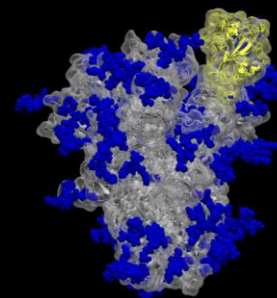
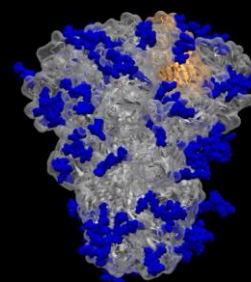
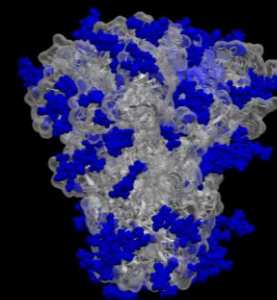
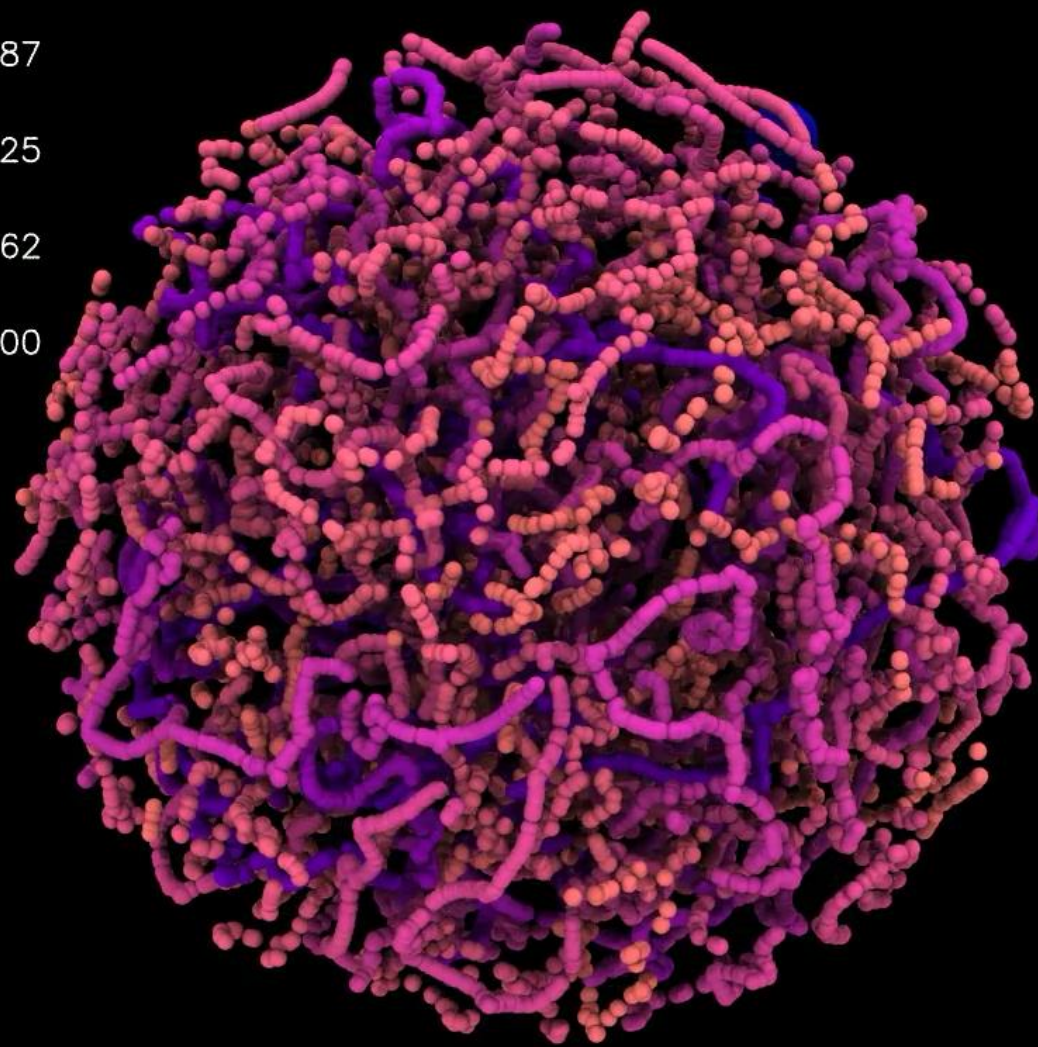
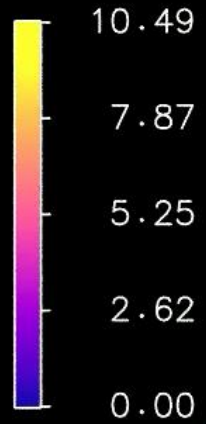


- **VAE**: larger memory footprint and longer training times
- **AAE**: can scale to much larger protein sizes and far more efficient in training time
 - linear increase in memory utilization
 - almost constant cost in training time (better scaling)
- Machine learning for protein folding and dynamics. Current Opinion in Structural Biology, (2020).
- Discovering protein conformational flexibility through artificial intelligence-aided molecular dynamics. Journal of Physical Chemistry (2019).
- Reinforcement learning based adaptive sampling: Reaping rewards by exploring protein conformational landscapes. The Journal of Physical Chemistry B (2018).

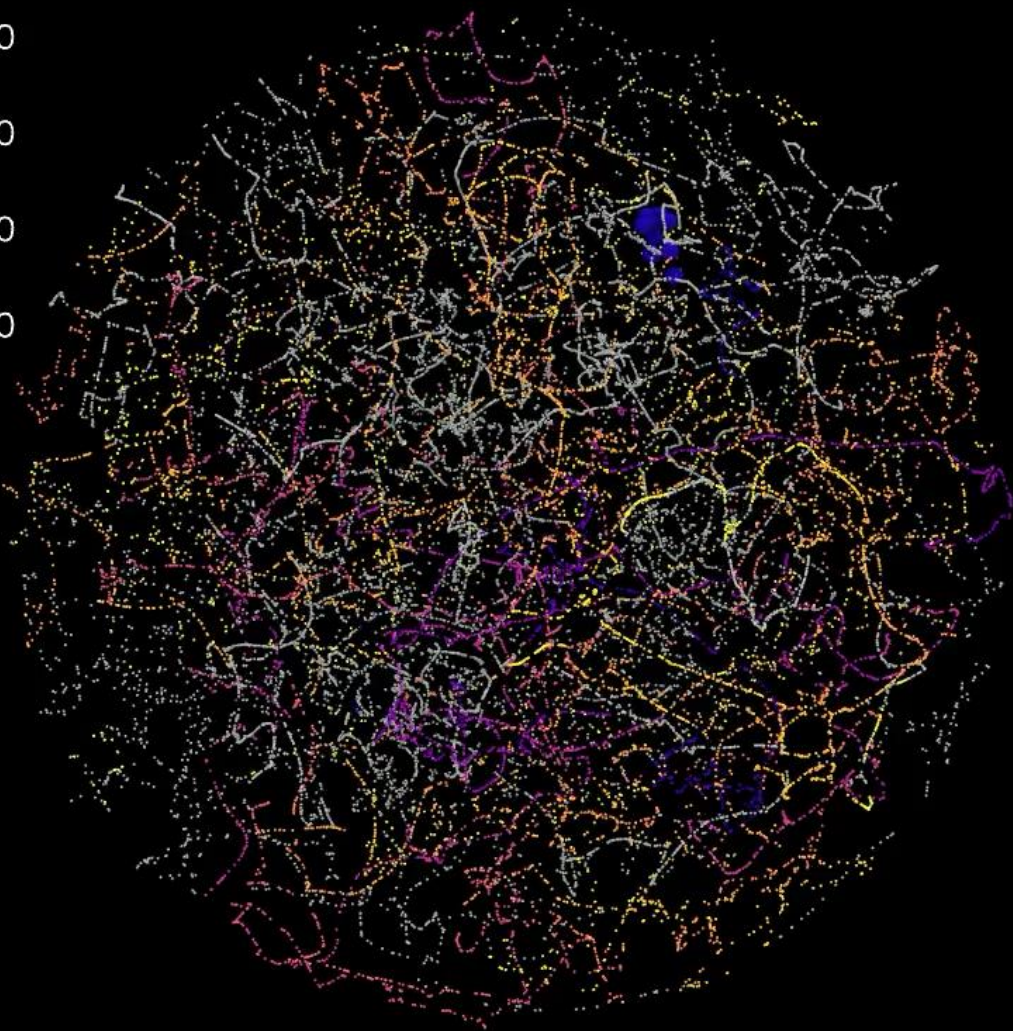
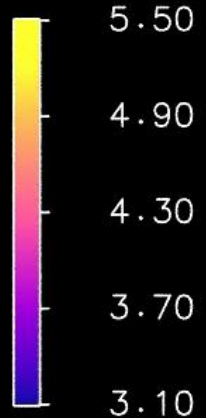
RMSD (Angstroms)



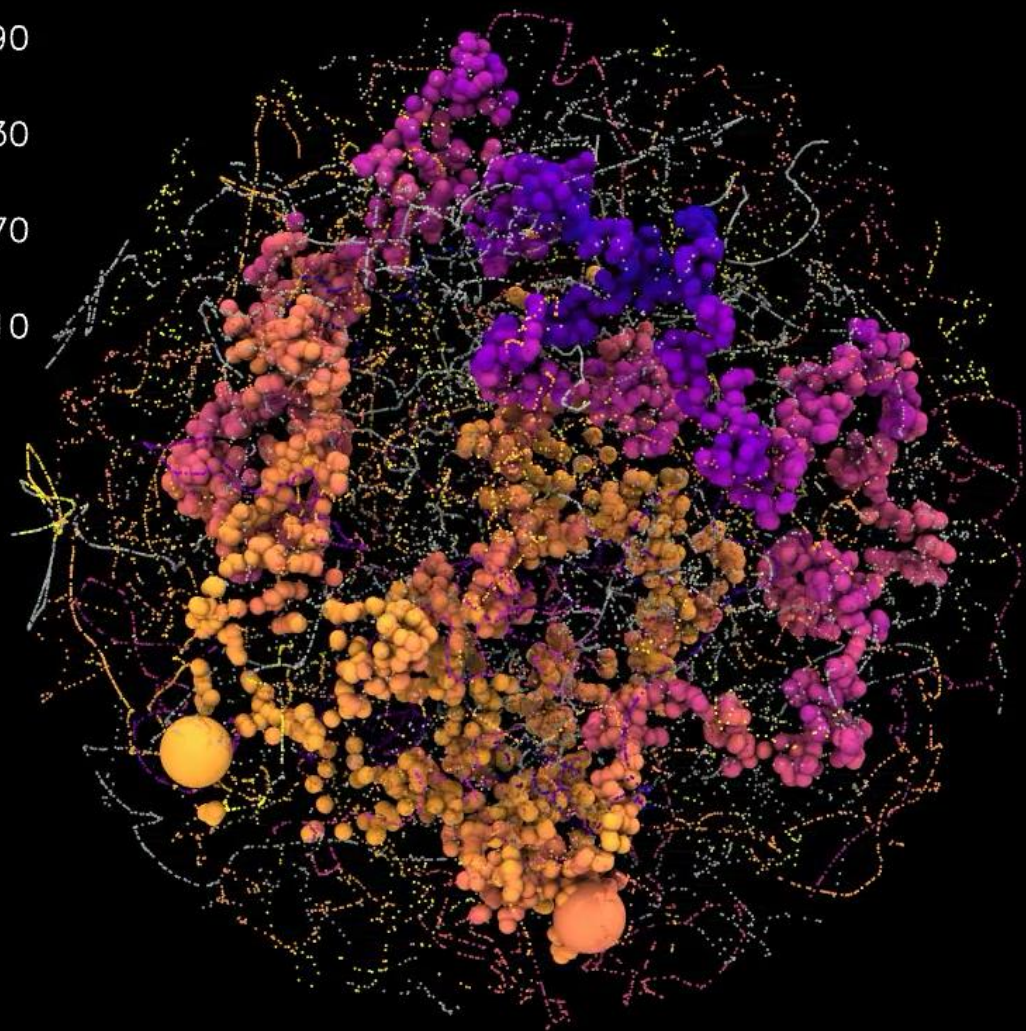
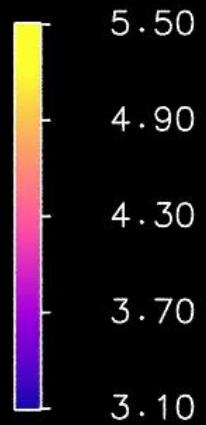
RMSD (Angstroms)



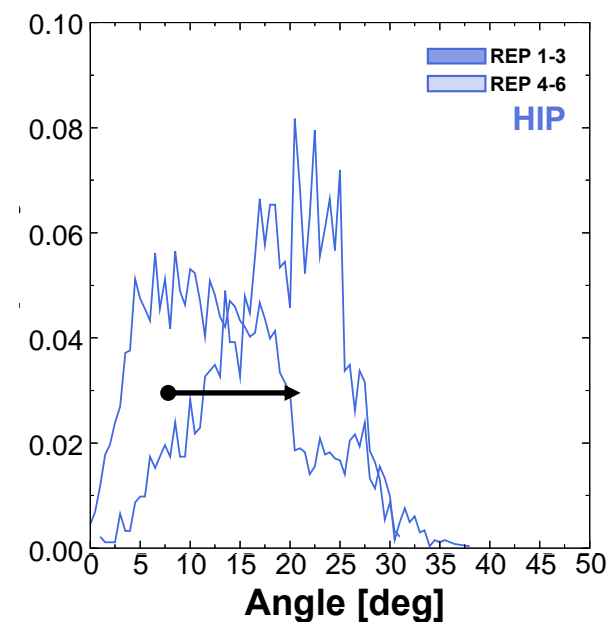
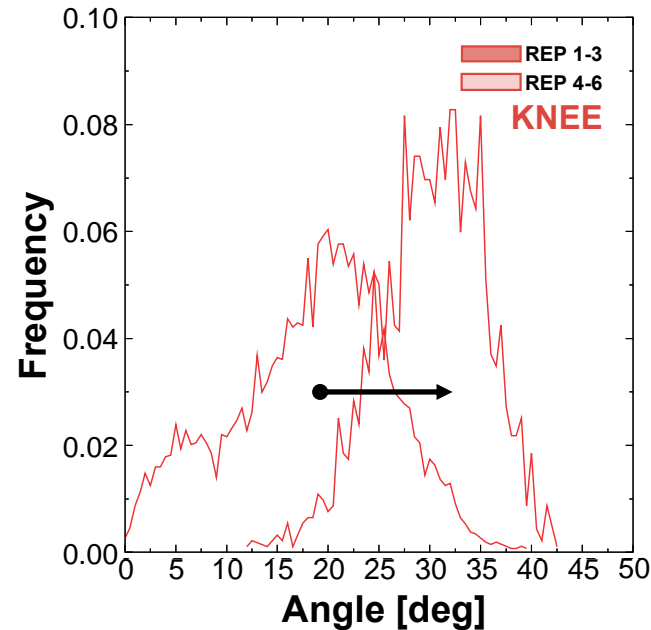
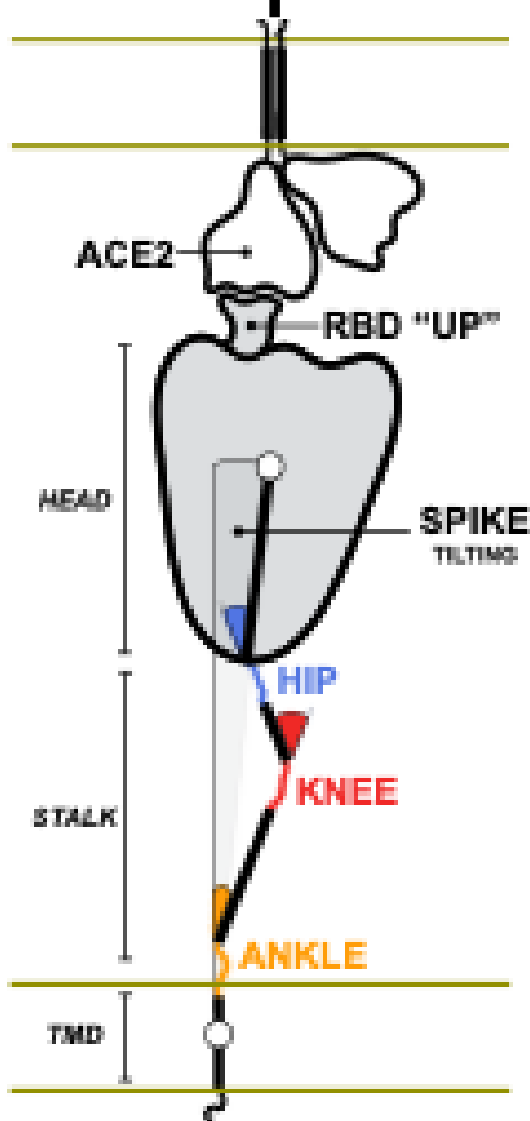
RMSD (Angstroms)



RMSD (Angstroms)

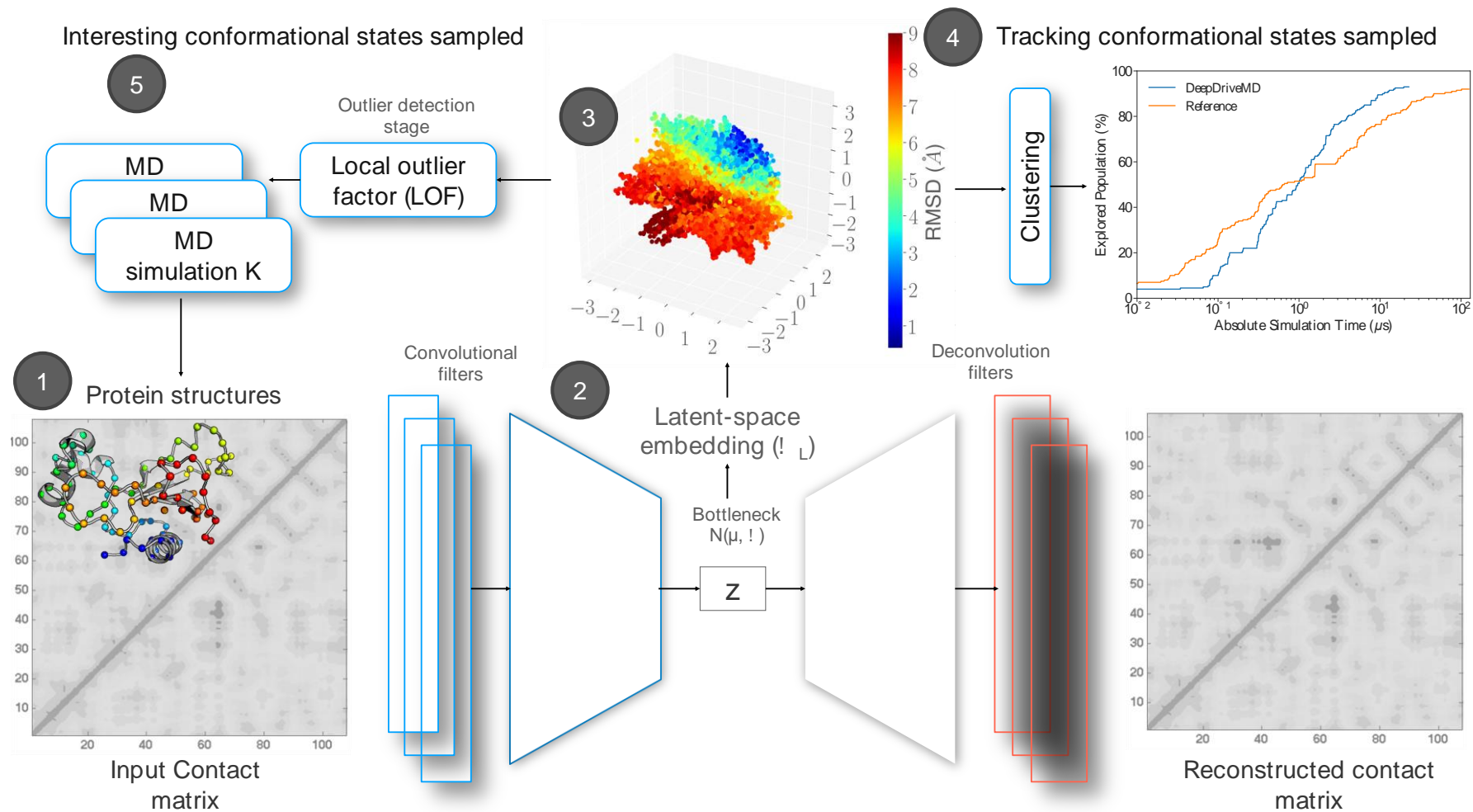


DeepDriveMD: Effective "Scientific" Performance



- Effective speedup of **$\approx 8.3\times$** sampling efficiency
 - without DeepDriveMD: 0.5 μs
 - with DeepDriveMD: 0.06 μs
- **Observed 25% more conformations of the knee bending in only 12% of the time!**
- Has been scaled to 1024 nodes of Summit for large ensembles

Enabling streaming AI/ML with multiscale simulations



Cerebras CS-1: A 15 RU System for Training & Inference in the Data Center

Powered by the Cerebras Wafer Scale Engine (WSE):

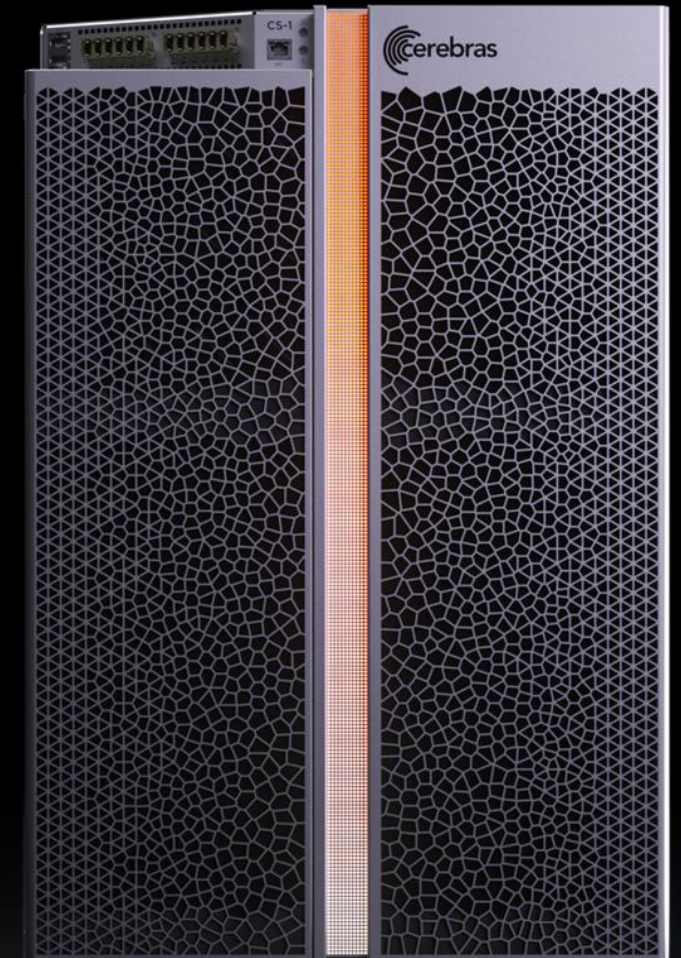
- **400,000** AI optimized cores
- **18 GB** on chip memory—all 1 clock cycle from the cores,
 - 4 Billion parameters for training (FP 16); 16B inference (8int)
- **9 PByte/s** memory bandwidth
- **100 Pbit/s** fabric bandwidth

System IO: **12 x 100 GbE**

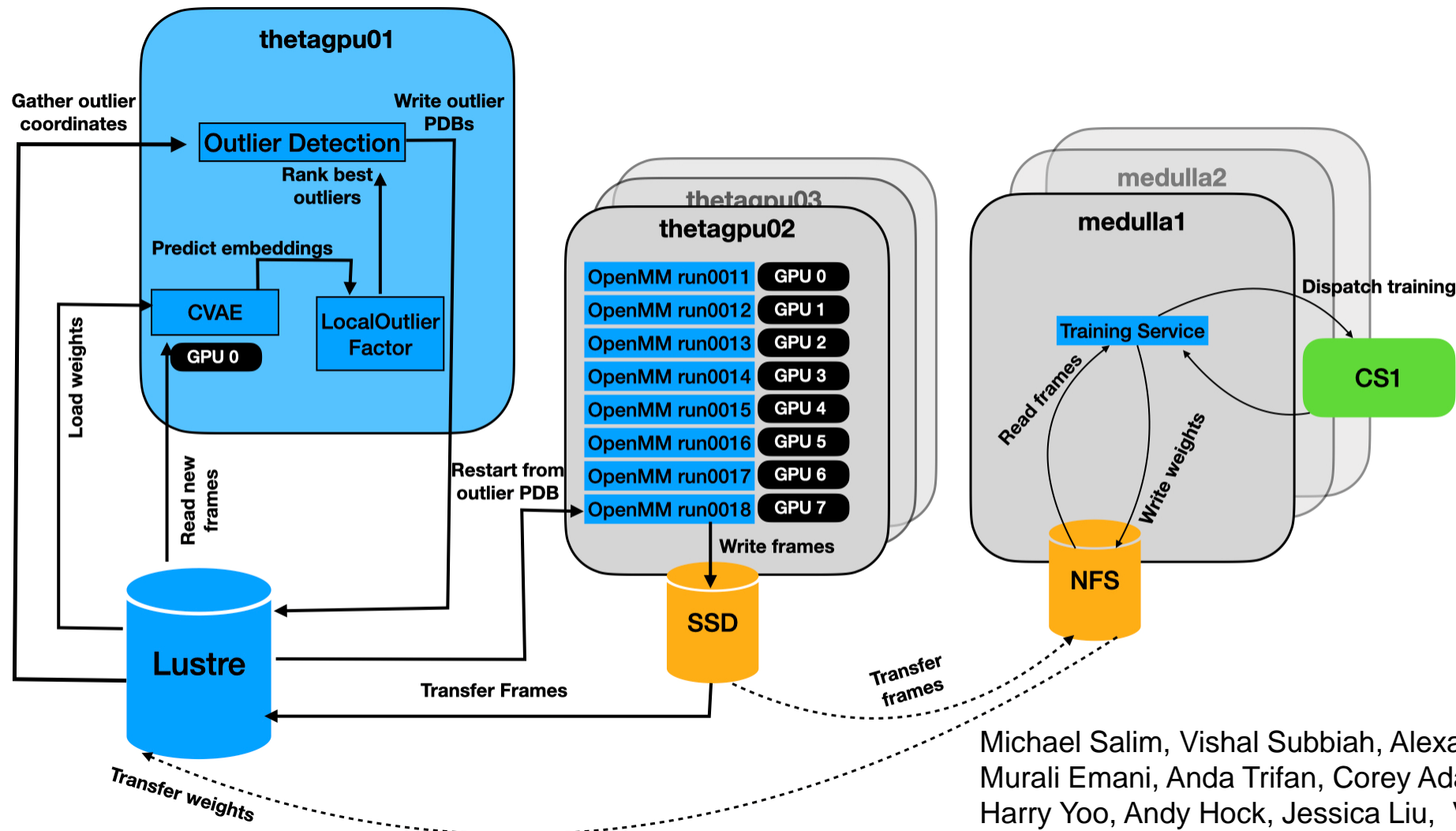
System power: **20 kW**

Ingests TensorFlow, PyTorch, etc.

Courtesy: Cerebras Systems Inc.

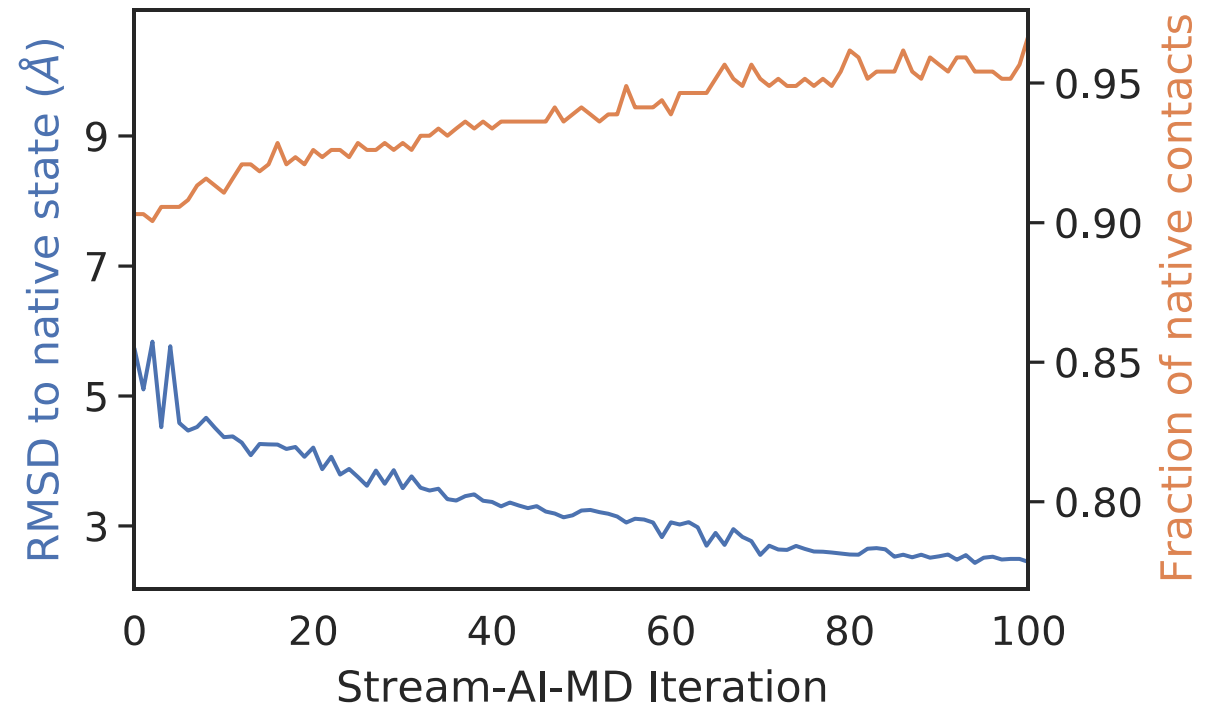
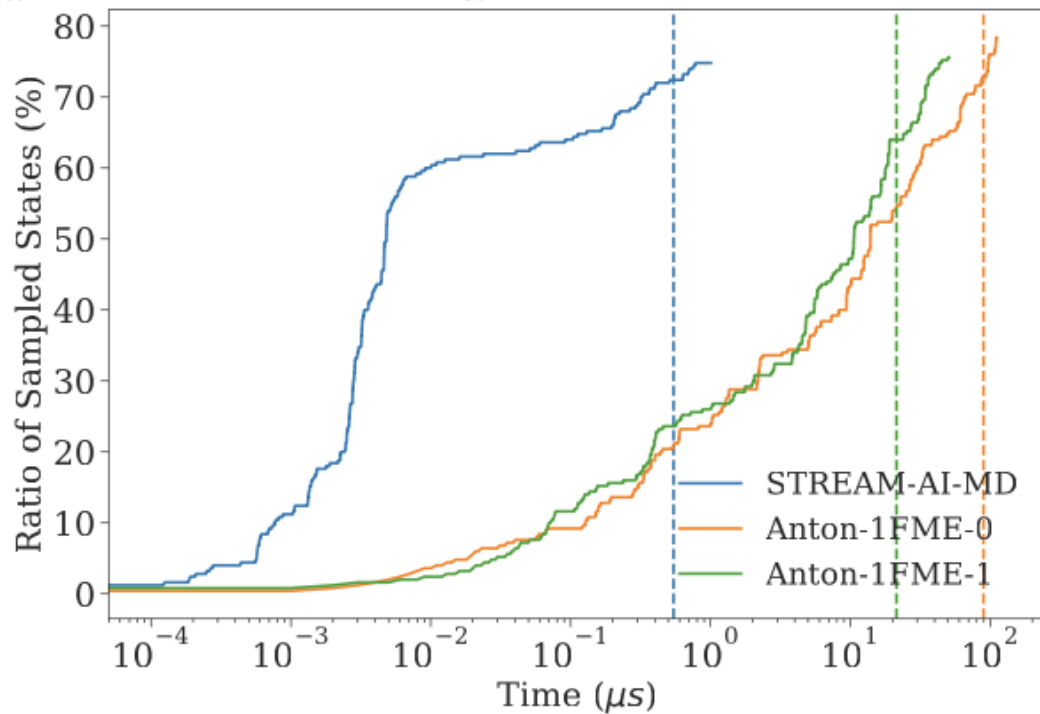


Bringing together heterogenous hardware to enable streaming analysis

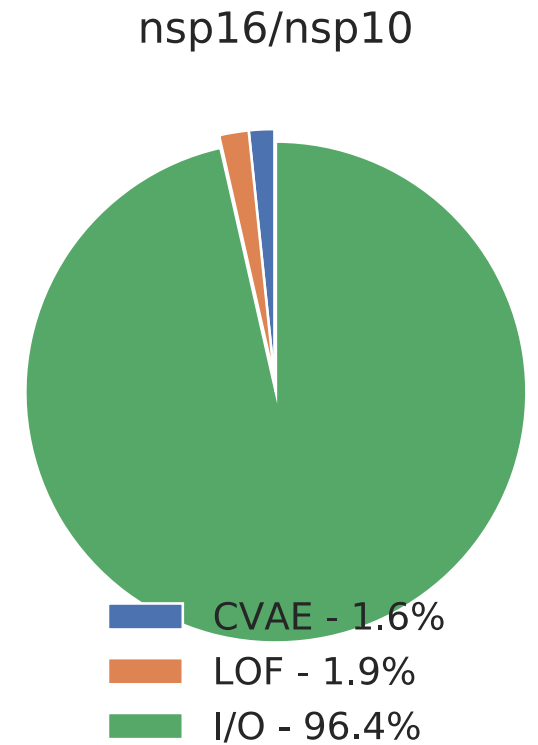
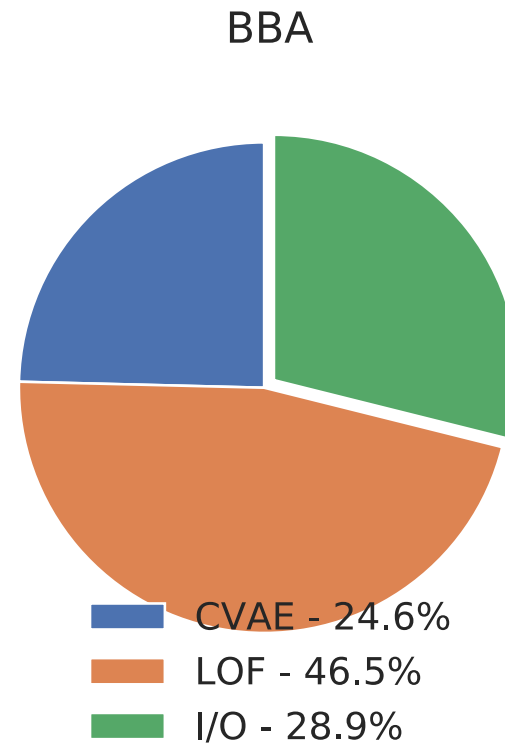
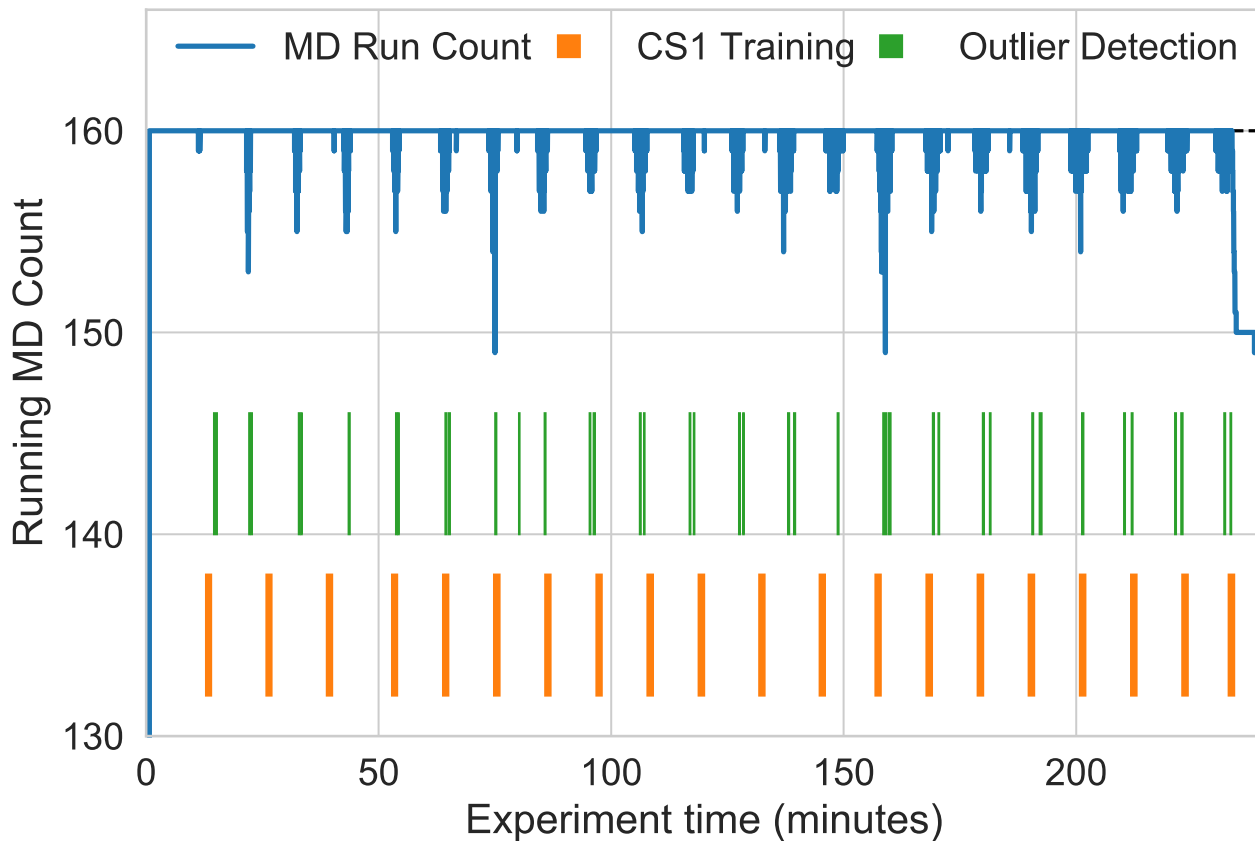


Michael Salim, Vishal Subbiah, Alexander Brace, Heng Ma, Murali Emani, Anda Trifan, Corey Adams, Thomas Uram, Harry Yoo, Andy Hock, Jessica Liu, Vernkat Vishwanath, Arvind Ramanathan

Stream-AI-MD enables at least 2 orders of magnitude faster sampling of folded states

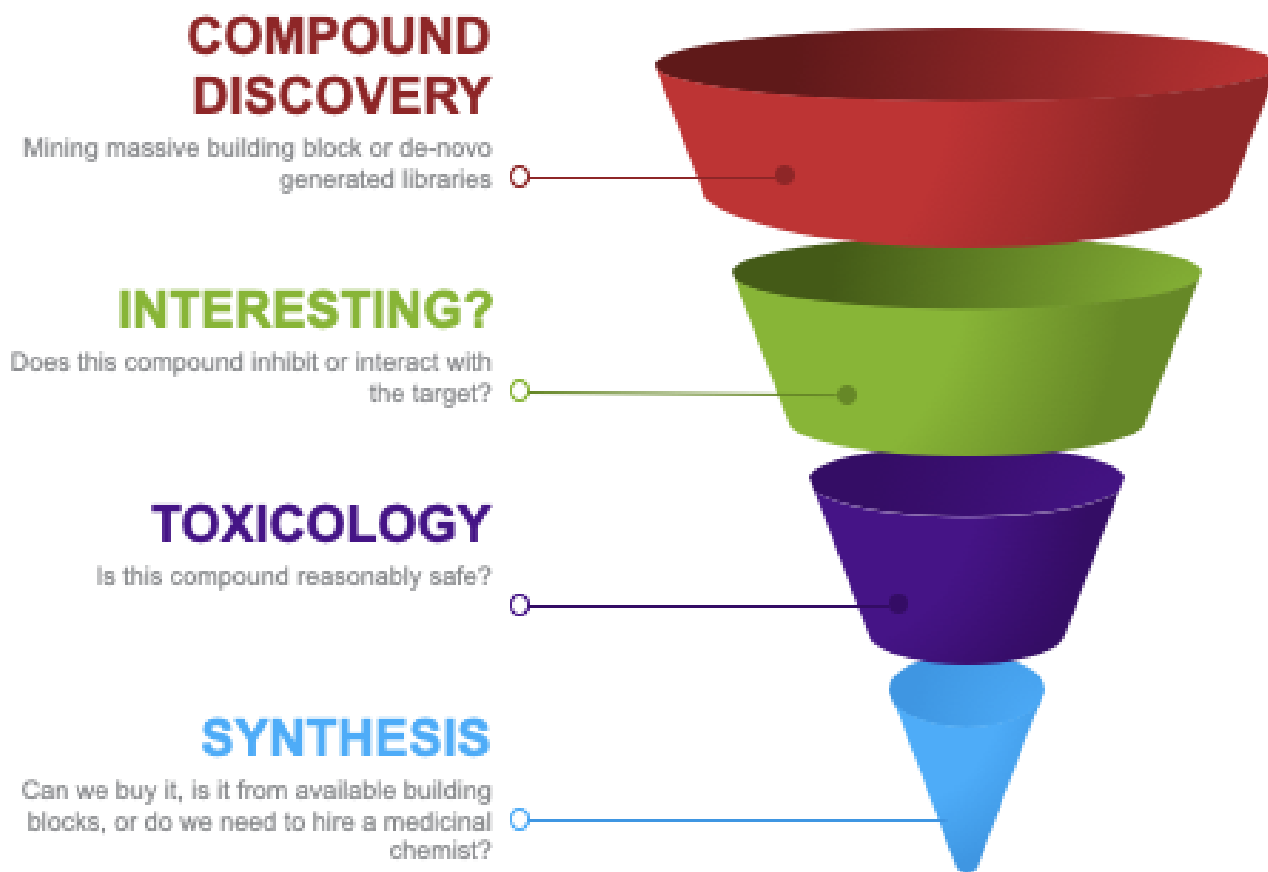


Utilization of hardware resources can vary depending on how tasks are scheduled



Outline (2)

10^{60} estimated drug-like compounds

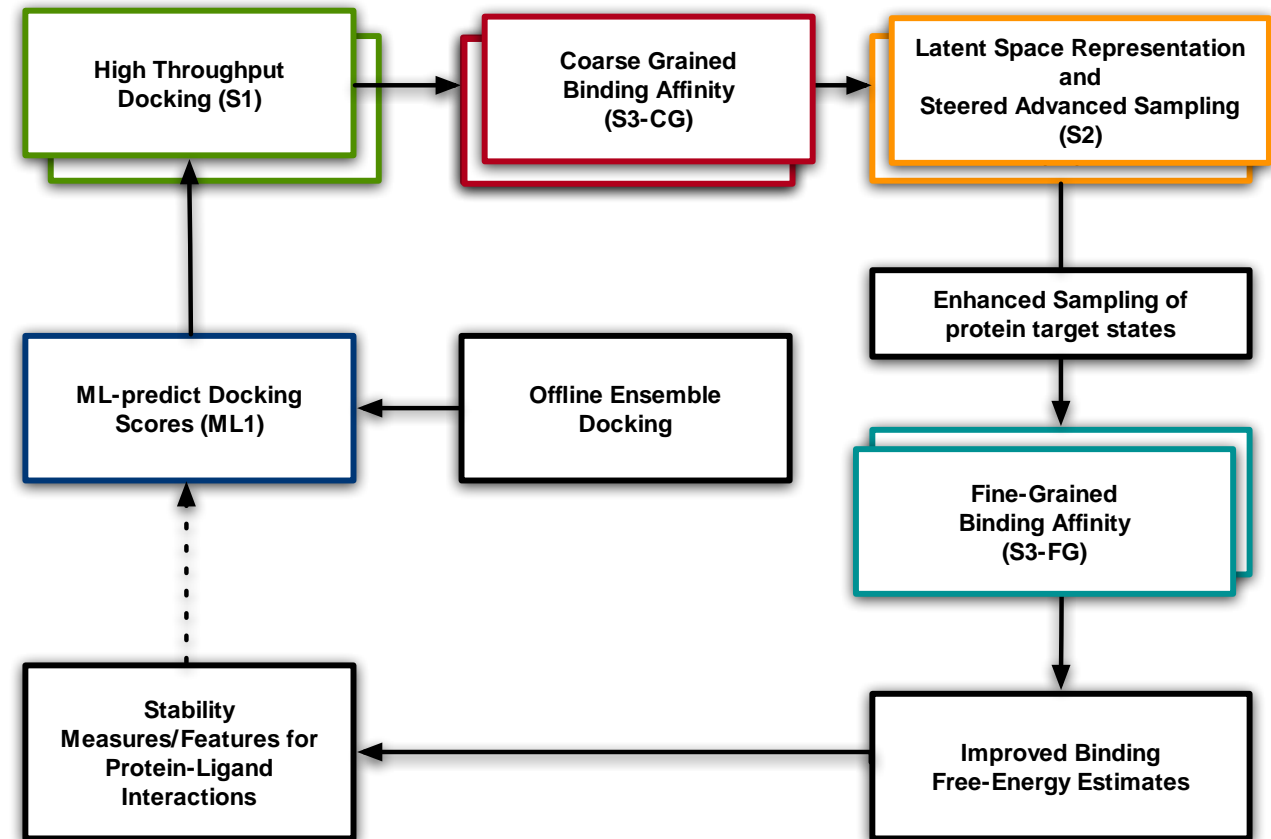


How to search billions of molecules to find drug candidates?

Improving docking and finding better ligands that bind to SARS-COV-2 proteome

Multi-stage campaign employed to select promising drug candidates:

- **Stage-1:** High-throughput ensemble docking to identify small molecules (“hits”)
- **Stage-2:** AI-driven Molecular Dynamics for modeling specific binding regions and understanding mechanistic changes involving drugs
- **Stage-3:** Binding Free Energy calculations of promising leads and (expensive) lead optimization



Aymen Al Saadi, Dario Alfe, Yadu Babuji, Agastya Bhati, Ben Blaiszik, Thomas Brettin, Ryan Chard, **Anda Trifan**, Alex Brace, Austin Clyde, Ian Foster, Tom Gibbs, Kristopher Keipert, Thorsten Kurth, Dieter Kranzlmüller, Hyungro Lee, Heng Ma, Andre Merzky, Gerald Matthias, Alexander Partin, Junqi Qiu, Ashka Shah, Abraham Stern, Li Tan, Mikhail Titov, Aristedis Tsaris, Matteo Turilli¹, Huub Van Dam, Shunzhou Wan, David Wifling, Shantenu Jha*, Peter Coveney*, Rick Stevens*, Arvind Ramanathan*

Why not dock every available compound?

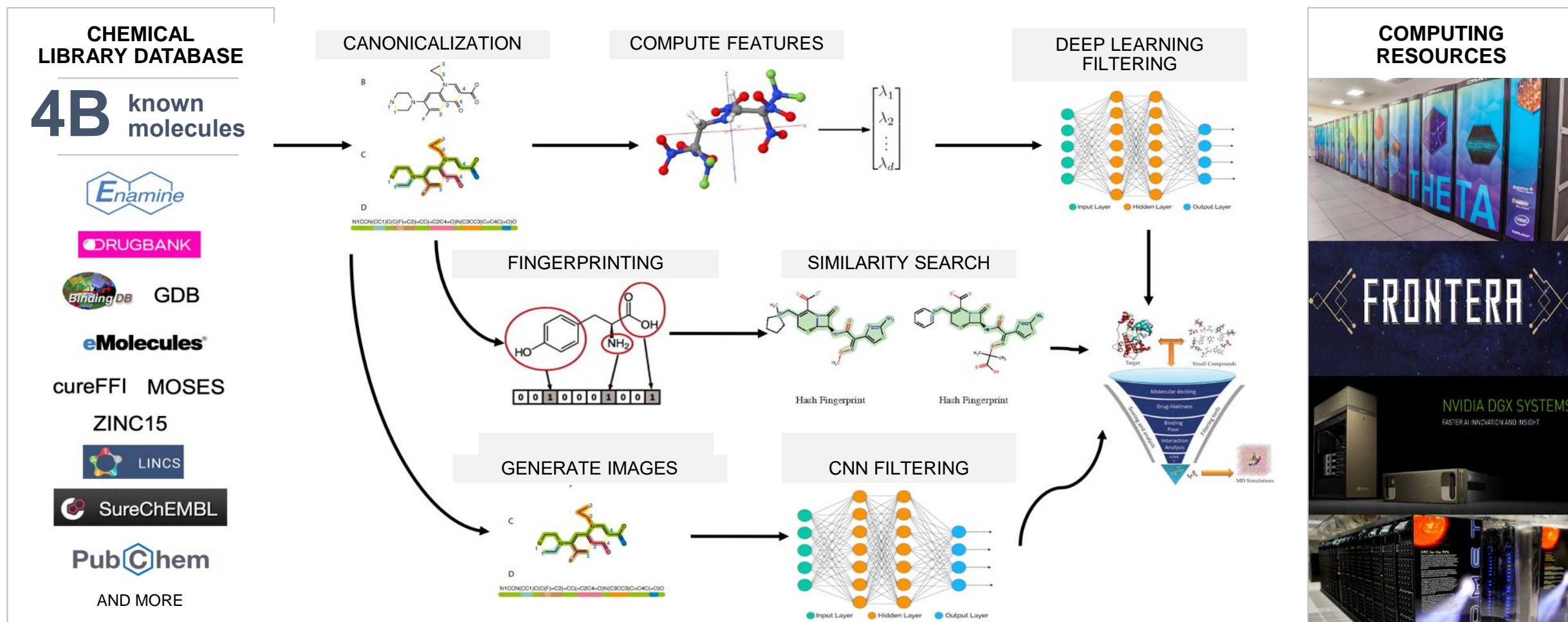
Table 3: Throughput and performance measured as peak flop per second (mixed precision, measured over short but time interval) per Summit node (6 NVIDIA V100 GPU).

| Comp. | #GPUs | Tflop/s | Throughput |
|-------|-------|---------|------------------|
| ML1 | 1536 | 753.9 | 319674 ligands/s |
| S1 | 6000 | 112.5 | 14252 ligands/s |
| S3-CG | 6000 | 277.9 | 2000 ligand/s |
| S3-FG | 6000 | 732.4 | 200 ligand/s |

- S1 \rightarrow $O(15,000)$ ligands/sec on 6 GPUs \rightarrow all of Summit will still take $\sim 6.8 - 8$ hours to compute!!
- This is on one receptor \rightarrow 100 receptors is not feasible

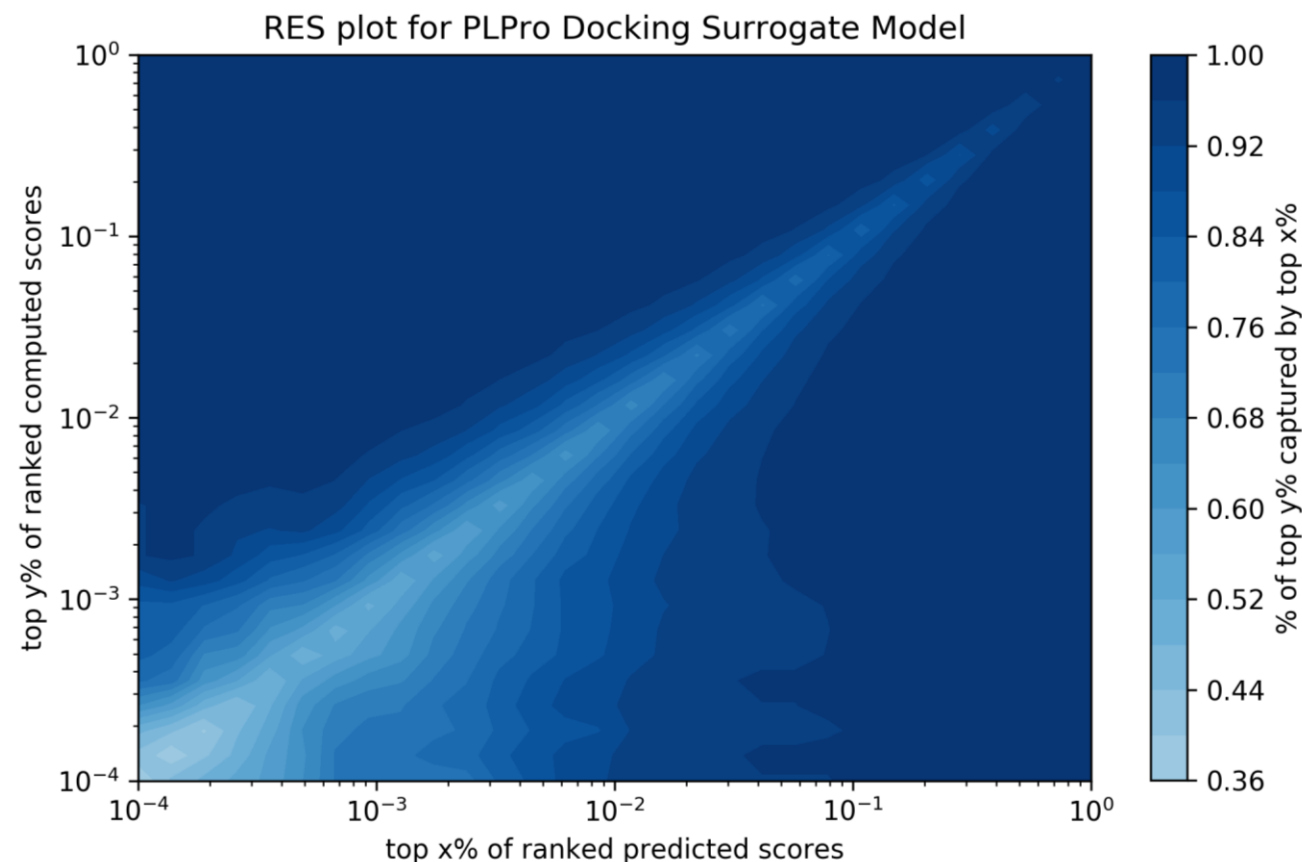
The COVID'19 data pipeline:

Developing machine readable datasets for small molecule libraries



ML to the rescue! Increased scientific throughput for virtual screening

- Instead of docking or predicting the docking pose, predict:
 - the docking score: a regression problem
 - whether a molecule will bind to a given protein target
- ML problem formulation: how many compounds can we find at the top-ranking list given some training data?
 - still uses the regression problem
 - instead of ranking we provide a bound for saying how many compounds we need to dock before we get "true hits"
- Leverage image-based models (CNNs on image with rotation invariant formulations) that are well optimized



A. Clyde, R. Stevens, Regression Enrichment Surfaces,
<https://arxiv.org/abs/2006.01171>

https://github.com/aclyde11/regression_enrichment_surface

Computational performance

| Use Case | Platform | Application | Nodes | Pilots | Ligands [$\times 10^6$] | Utilization | Docking Time [sec] | | | Docking Rate [$\times 10^6$ docks/hr] | | |
|---------------------------------------|----------|--------------|-------|--------|---------------------------|----------------|--------------------|--------|------|--|------|------|
| | | | | | | | min | max | mean | min | max | mean |
| 1 | Frontera | OpenEye | 128 | 31 | 370 | 89.6% | 0.1 | 3582.6 | 28.8 | 0.2 | 17.4 | 5.0 |
| 2 | Frontera | OpenEye | 3850 | 1 | 125 | 95.5% | 0.1 | 833.1 | 25.1 | 16.0 | 27.5 | 19.1 |
| 3 <input checked="" type="checkbox"/> | Summit | AutoDock-GPU | 1000 | 1 | 57 | $\approx 95\%$ | 0.1 | 263.9 | 36.2 | 10.9 | 11.3 | 11.1 |

Table 1: WF1 use cases. For each use case, RAPTOR uses one pilot for each receptor, computing the docking score of a variable number of ligands to that receptor. OpenEye and AutoDock-GPU implement different docking algorithms and docking scores, resulting in different docking times and rates. However, resource utilization is $\geq 90\%$ for all use cases.

Table 2: Normalized computational costs on Summit.

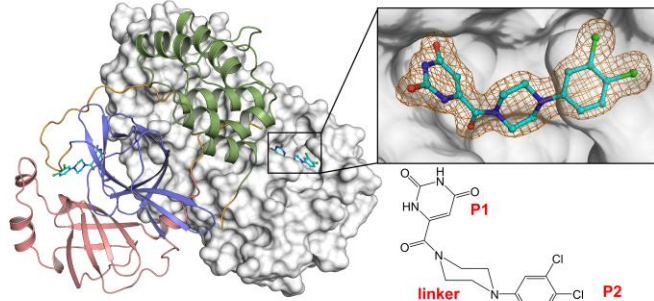
| Method | Nodes per ligand | Hours per ligand (approx) | Node-hours per ligand |
|-------------------|------------------|---------------------------|-----------------------|
| Docking (S1) | 1/6 | 0.0001 | ~ 0.0001 |
| BFE-CG (S3-CG) | 1 | 0.5 | 0.5 |
| Ad. Sampling (S2) | 2 | 2 | 4 |
| BFE-FG (S3-FG) | 4 | 1.25 | 5 |
| BFE-TI | 64 | 10 | 640 |

Table 3: Throughput and performance measured as peak flop per second (mixed precision, measured over short but time interval) per Summit node (6 NVIDIA V100 GPU).

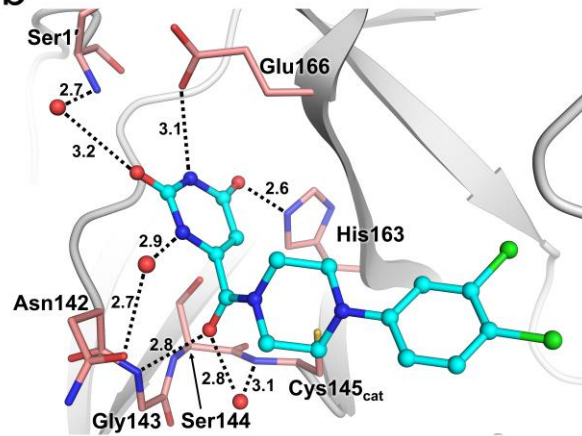
| Comp. | #GPUs | Tflop/s | Throughput |
|-------|-------|---------|------------------|
| ML1 | 1536 | 753.9 | 319674 ligands/s |
| S1 | 6000 | 112.5 | 14252 ligands/s |
| S3-CG | 6000 | 277.9 | 2000 ligand/s |
| S3-FG | 6000 | 732.4 | 200 ligand/s |

Our workflow results in better binding compounds ...

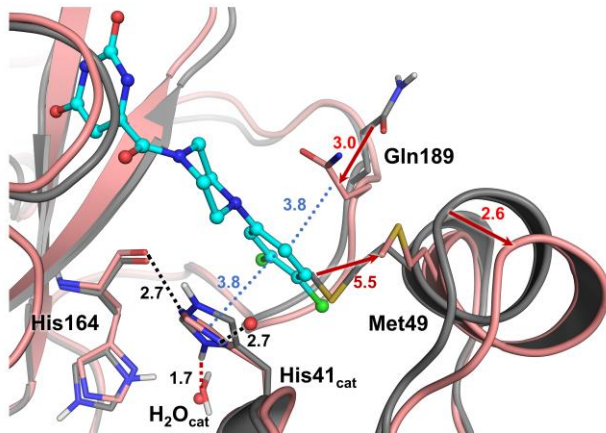
a



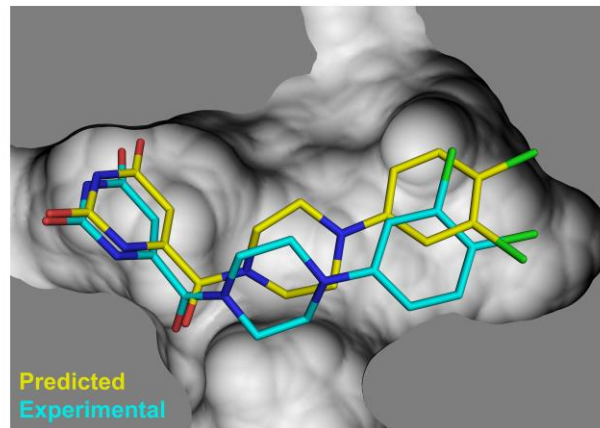
b



c



d



- From the 1000 compounds were ordered for whole-cell assays, ~50 of compounds show viral inhibition activity
- Several compounds have already been processed for X-ray crystallography efforts (at Argonne and NSLS-II)
- Synthetic chemistry efforts are being driven across labs to either optimize compounds

Impacting SARS-CoV-2 Medical Therapeutics

- Scale of operation:
 - $\sim 10^{11}$ docking calculations using OpenEye and Autodock in ratio 10:1
 - Thousands of DeepDriveMD calculations over multiple platforms (Summit, Lassen, ...)
 - 5×10^4 Binding Free Energy Calculations across machines
 - 2.5×10^6 node-hours (equal to ~ 25 days of 100% of Summit)
 - Assuming 5-year lifetime of Summit at \$500M \rightarrow \$6M cost of computing!
- For S1, we estimate 1.25×10^6 node hours (lower bound)
 - Peak Performance: ~ 4000 nodes for docking studies on Frontera (06 Sep 2020),
- Robust and Extensible Computational Infrastructure and Capabilities
 - Campaign -- 24x7 operation over multiple heterogeneous resources
 - AI-methods & Software Systems can be extended to ATOM, and other drug discovery pipelines
 - Extending computational infrastructure to NSLS-II covalent inhibitors of cysteine proteases

Funding and acknowledgements

- Everyone in the team (all ~300)
- Computing support:
 - ALCF, OLCF
 - TACC, SDSC, IU
 - HPC Consortium
- Funding acknowledgement:
 - DOE National Virtual Biotechnology Laboratory (NVBL)
 - Argonne internal funding (LDRD)
 - DOE Exascale computing project (Cancer Deep Learning Environment)

THANK YOU!!!

ramanathana@anl.gov